



Norwegian University of
Science and Technology

MultiBooster instability and surge

Ustabilitet og surge i MultiBooster

Richard H. Kringlebotten

Master of Energy and Environmental Engineering

Submission date: June 2016

Supervisor: Lars Eirik Bakken, EPT

Co-supervisor: Alberto Serena, EPT
Øyvind Hundseid, EPT

Norwegian University of Science and Technology
Department of Energy and Process Engineering

EPT-M-2016-73

MASTER THESIS

for

Student Richard Kringlebotten

Spring 2016

MultiBooster instability and surge*Ustabilitet og surge i MultiBooster***Background**

The turbomachinery industry focus has lately turned to multiphase boosting where the technology need is steadily increasing. Aker Solutions, a company at the leading edge of technology in the field of subsea pump systems, is extending its product portfolio with new multiphase pump technologies to improve production of gas rich fields through use of multiphase boosting.

Instability and surge are important issues in multiphase boosters, affecting both performance and booster system stability. Accurate study of the flow mechanisms is required to understand the fundamentals and thus lays the foundation for design improvements. The novel facility installed at the Thermal Energy Department provides an excellent optical access to the pump channels, allowing detailed visual investigations and study of characteristic flow phenomena during instability and surge.

Objective and tasks

The main objective is to document “state-of-the-art” technology related to multiphase boosters instability and surge mechanisms. The approach should be based on a review of previous approaches to define and describe surging, image processing metrology (at least to characterize the bubbles size and phase slip during surging) and also some analysis to relate pressure pulsations to flow mechanisms. A close cooperation with the PhD project “MultiBooster Performance” is required.

1. Document the operating condition inception and evolution, and the two-phase flow instabilities involved
2. Evaluate image-based metrology to assess and document the phase slip. Comparison with available correlations should be included.
3. Develop a “surging-inception detection method” through the correlation of different measurements which show characteristic variations as this condition is approached.

-- ” --

Within 14 days of receiving the written text on the master thesis, the candidate shall submit a research plan for his project to the department.

When the thesis is evaluated, emphasis is put on processing of the results, and that they are presented in tabular and/or graphic form in a clear manner, and that they are analyzed carefully.

The thesis should be formulated as a research report with summary both in English and Norwegian, conclusion, literature references, table of contents etc. During the preparation of the text, the candidate should make an effort to produce a well-structured and easily readable report. In order to ease the evaluation of the thesis, it is important that the cross-references are correct. In the making of the report, strong emphasis should be placed on both a thorough discussion of the results and an orderly presentation.

The candidate is requested to initiate and keep close contact with his/her academic supervisor(s) throughout the working period. The candidate must follow the rules and regulations of NTNU as well as passive directions given by the Department of Energy and Process Engineering.

Risk assessment of the candidate's work shall be carried out according to the department's procedures. The risk assessment must be documented and included as part of the final report. Events related to the candidate's work adversely affecting the health, safety or security, must be documented and included as part of the final report. If the documentation on risk assessment represents a large number of pages, the full version is to be submitted electronically to the supervisor and an excerpt is included in the report.

Pursuant to "Regulations concerning the supplementary provisions to the technology study program/Master of Science" at NTNU §20, the Department reserves the permission to utilize all the results and data for teaching and research purposes as well as in future publications.

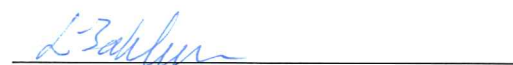
The final report is to be submitted digitally in DAIM. An executive summary of the thesis including title, student's name, supervisor's name, year, department name, and NTNU's logo and name, shall be submitted to the department as a separate pdf file. Based on an agreement with the supervisor, the final report and other material and documents may be given to the supervisor in digital format.

- Work to be done in lab (Water power lab, Fluids engineering lab, Thermal engineering lab)
 Field work

Department of Energy and Process Engineering, 13. January 2016



Olav Bolland
Department Head



Lars E Bakken
Academic Supervisor

Research Advisors:
Alberto Serena
Øyvind Hundseid

Preface

This master's thesis is written at the Department of Energy and Process Engineering at NTNU during the spring semester of 2016.

I would like to thank my supervisor, Lars Eirik Bakken, for his guidance throughout the project. Next, a huge thanks to my co-supervisor, PhD candidate Alberto Serena, for all technical discussions and the experimental work performed. I would also thank Ole Jørgen Nydal professor in multi-phase pipeflow at NTNU for the technical discussions.

Richard Helgø Kringlebotten

Trondheim, June 13, 2016

Abstract

Industry has lately turned the focus on subsea processing as a tool to enable new developments where the technology needs are increasing. Multiphase pumping ("boosting") plays a key role in the increase of production and in oil and gas recovery. In addition, the technology has shown to be more profitable and environmental friendly compared to conventional methods, due to longer tie-back distances and the potential of zero gas flaring. However, the presence of gas leads to unwanted flow regimes generating additional performance losses and system instabilities.

Safe and reliable operation requires a deep understanding of the physical mechanisms causing the unstable behavior. The main objective of the thesis has been to explore the multiphase booster instability and surging mechanisms to give an improved insight of the main influencing flow mechanisms.

A literature study has been performed, reviewing previous studies considering surging in multiphase pumps. In addition, phase slip and other related mechanisms have been studied through bubble tracking and available correlations. Data processing and direct flow visualization with a high-speed camera have been employed in experimental tests. Additionally, a data processing system have been utilized in order to relate pressure pulsations to flow mechanisms.

An extensive test campaign has been conducted through the test facility in the Thermal Energy Department Laboratory at NTNU. The facility features a mixed-flow rotodynamic single-stage multiphase pump, reproducing the full scale, MultiBooster, by Aker Solutions at Tranby (Oslo). The transparent pump casing permits an excellent optical access of the hydraulic channels, which allows a visual study of the flow field behavior. All tests have been performed at atmospheric inlet pressure, where gas volume fractions, flow rates, and rotational speeds are the varying parameters.

Characteristic multiphase flow phenomena have been analyzed through flow visualization, bubble tracking, and data processing. The phenomena have shown to affect the machine negatively, due to the increased pressure variations and channel obstructions. The experimental work indicates that, bubble coalescence, gas pockets, phase slip, "empty-of-gas" channels, and recirculation zones plays a major role during the unsteady machine operation. The phenomena show an intermittent behavior, dependent on the operating condition and the specific pump design. As the surging is approached, the overall flow field irregularities show to intensify, accompanied with strong pressure variations. Moreover, this correlation has formed a foundation for detecting the surging inception, and will be presented in this thesis.

Sammendrag

Industrien har i senere tid rettet fokuset mot subsea produksjon hvor etterspørselen etter ny teknologi er økende. Flerfase pumping ("boosting") spiller en viktig rolle for økt produksjon og opphenting av olje- og gassproduksjon. Teknologien har vist seg å være lønnsom og mer miljøvennlig sammenlignet med tidligere metoder, grunnet potensialet for null fakkeltutslipp og lengre tilknytningslinjer. Gass vil dog føre til uønskede strømningsregimer, samt høyere ytelsestap og ustabiliteter i systemet.

Sikker drift forutsetter dyp forståelse om de forårsakende mekanismene. Hovedmålet med denne oppgaven er å utforske ustabiliteter og surging i flerfase booster for å bidra til en økt forståelse av hovedinteragerende strømningsmekanismer.

Relevante studier utført tidligere på ustabiliteter og surging i flerfasepumper er gjennomgått i form av et litteraturstudie. I tillegg, så har fase "slip" og relaterte mekanismer blitt studert gjennom boble "tracking" og tilgjengelige korrelasjoner. Eksperimentelt arbeid er gjennomført ved hjelp av et avansert data-målesystem og høyhastighets-kamera. En måte for å analysere trykkdata opp mot opptakene er utført ved et data-prosesserings-system som synkroniserer trykkmålinger opp mot strømningsmekanismer.

En omfattende testplan har blitt gjennomført via test-riggen lokalisert i termisk laboratorium på NTNU. Riggen består av en ett-trinns "mixed-flow" sentrifugalpumpe som gjengir en nedskalert versjon av Aker Solutions' "MultiBooster". Det gjennomskjete pleksiglasset tillater innsyn til de hydrauliske kanalene. Noe som gjør det mulig å studere strømningsfenomenene ved hjelp av visualiseringsmetoder. Alle tester er utført ved atmosfærisk innløpstrykk for forskjellige verdier av volumetrisk gassfraksjon (GVF), volumstrøm og rotasjons hastighet.

Karakteristiske flerfase-fenomen har blitt analysert via strømnings-visualisering, boble "tracking" og data-prosessering. Koalisering av bobler, lommer av gass, fase "slip", "empty-of-gas" rotorkanaler, samt områder preget av resirkulasjonsstrømning har vist seg å være av høy interesse med hensyn til trykkvariasjoner og ustabiliteter i pumpesystemet. Strømningsfenomenene har vist å avhenge av strømningsstilstand og pumpedesign. Innflytelsen er gjenkjent som mer intens ettersom pumpetilstanden nærmer seg surging. Strømnings-visualisering, i samsvar med en økende trend av trykkvariasjoner, har bidratt til å detektere surging gjennom et kriterium, som vil bli presentert i oppgaven.

Contents

Preface	i
Abstract	ii
Sammendrag	iii
Nomenclature	vii
1 Introduction	1
1.1 Background	1
1.2 Challenges	3
1.3 Scope of Thesis	3
1.4 Limitations	3
1.5 Report Structure	4
2 Fundamental Theory	5
2.1 Pump Theory	5
2.2 Multiphase flow	8
2.2.1 Two-Phase Fundamentals	8
2.2.2 Two-phase Modeling	10
2.2.3 Flow Pattern	11
2.3 Summary	13
3 Visual Flow Analysis	15
3.1 Associated Phase Slip Mechanisms	15
3.1.1 Rotating Channel Flow	16
3.1.2 Transversal Acceleration Field	18
3.1.3 Bubble Behavior	18
3.2 Available Phase Slip Correlations	22
3.3 Evaluation of Image-Based Metrology	24
3.4 Summary	26
4 Surging in Multiphase Pumps	29
4.1 Previous Investigations	29
4.2 Summary	32

5	Test Facility and Experimental Method	33
5.1	Test Facility	34
5.1.1	Risk Assessment and Operational Limitations	35
5.2	Visualization Equipment	35
5.2.1	Direct Flow Visualization	36
5.3	Data Acquisition Equipment	37
5.3.1	Pressure Sensors	37
5.3.2	Data Logging System	38
5.3.3	Data Processing	39
5.4	Experimental Procedure	39
5.5	Rig Evaluation and Error Sources	40
6	Results and Discussions	43
6.1	Multiphase Booster Instability	43
6.1.1	Surging Inception	44
6.1.2	Bubble Coalescence and Gas Pockets	47
6.1.3	Empty-of-Gas Channel	51
6.1.4	Diffuser Flow Investigations	55
6.2	Surging Detection	57
6.2.1	Fundamental Variables	57
6.2.2	Surging Detection	58
6.2.3	Multiphase Booster Surging Zone	61
6.3	Summary	63
7	Conclusion	65
8	Recommended Work in Future Research	67
	Bibliography	69
	Appendices	73
A	P&ID & Instrumentation List	73
B	Graphs	76
C	Phase slip correlations for 1D pipe flow	77
D	Bubble Tracking	78
E	Gantt Diagram	79

Nomenclature

Symbols

\dot{m}	Mass flow	$[\frac{kg}{s}]$
A	Area	$[m^2]$
D	Diameter	$[m]$
d_p	Diameter particle	$[m]$
F	Force	$[N]$
g	Gravitational constant	$[\frac{m}{s^2}]$
H	Head	$[m]$
n	Pump speed	$[rpm]$
p	Pressure	$[bar]$
q^*	Fraction of nominal flow rate	$[\%]$
r	radius	$[m]$
U	Tip speed	$[\frac{m}{s}]$
V	Fluid absolute velocity	$[\frac{m}{s}]$
V_r	Relative phase velocity	$[\frac{m}{s}]$
W	Fluid relative velocity	$[\frac{m}{s}]$

Greek Symbols

β	Flow angle	$[^\circ]$
Δ	Differential value	

δ	Pressure variation fraction	[%]
γ	Slip ratio	
μ	Viscosity	$[\frac{kg}{sm}]$
ω	Angular rotational velocity	$[\frac{1}{s}]$
ρ	Density	$[\frac{kg}{m^3}]$
ρ^*	Density ratio	
σ	Surface tension	$[\frac{J}{m^2}]$

Subscripts

1	Inlet impeller
2	Outlet impeller
3	Outlet Diffuser
g	Gas
hom	Homogeneous
l	Liquid
m	Meridional velocity direction
max	Maximum
nom	Nominal
r	Relative
s	Superficial
th	Theoretical
tot	Total
TP	Two-phase
u	Peripheral velocity direction
w	Relative velocity direction

Abbreviations

<i>GMF</i>	Gas mass fraction	[%]
<i>GVF</i>	Gas volume fraction	[%]
CFD	Computational Fluid Dynamics	
DS	Deep surging	
ESP	Electrical submersible pump	
FFT	Fast Fourier transform	
HSE	Health, Security & Environment	
ISO	International Organization for Standardisation	
LDV	Laser Doppler Velocimetry	
LE	Leading edge	
NI	National Instruments	
ODE	Ordinary differential equation	
P&ID	Piping and Instrumentation diagram	
PFV	Photron FASTCAM Viewer	
PIV	Particle Image Velocimetry	
PMMA	Polymethylmethacrylate	
PS	Pressure side	
SS	Suction side	
TE	Trailing edge	
TP	Two-phase	
VF	Void fraction	

List of Figures

2.1	Circumferential and meridional view of a semi-axial impeller .	6
2.2	Velocity triangles inlet (left) and outlet (right)	7
2.3	Flow pattern map in a horizontal pipe, [36]	12
2.4	Flow regimes in a horizontal pipe [36]	12
3.1	Main influencing forces on an isolated bubble	17
3.2	Bubble shape regimes and transitions [15]	20
3.3	Bubble trajectory at 900 rpm and 70 % q^*	21
3.4	Experimental pressure increment for elongated flow versus homogeneous pressure prediction [24]	23
3.5	Flow visualization – rotating channel (upper row) and diffuser (bottom row) at different GVFs, 1200 rpm and 50% q^*	25
5.1	Test Rig at Thermal Energy Department, NTNU	33
5.2	Simplified P&ID	34
5.3	Placement of dynamic (PD) and static (PT) pressure sensors	37
5.4	LabVIEW screen	38
6.1	Approaching surging, 1% GVF	45
6.2	Approaching surging, 5% GVF	45
6.3	Surging onset, 10% GVF	46
6.4	Static inlet gas pocket at 900 rpm and 70% q^*	47
6.5	Surging at 1200 rpm and 70% q^*	49
6.6	Data processing – Surging at 1200 rpm and 70% q^*	49
6.7	Surging at 1200 rpm and 70% q^*	50
6.8	Empty-of-gas channel at 900 rpm and 70% q^* at surging onset	52
6.9	Data processing – 900 rpm and 70% q^* at surging	54
6.10	Diffuser Channel at Surging: 1800 rpm, 10% GVF and 50% q^*	55
6.11	Data processing at 1800 rpm, 10% GVF and 50% q^*	56
6.12	Flow fluctuations propagating back and forth within the pump	58
6.13	Performance curves approaching surging	59
6.14	Surging inception at partload and 1200 rpm	60
6.15	Surging inception at partload and 1500 rpm, 1800 rpm	61

6.16	Data points showing surging inception (dot point) and deep surging (cross point) conditions	62
1	P&ID	74
2	Instrumentation list	75
3	Surging detection	76
4	Surging detection	76
5	Bubble Tracking	78
6	Gantt Diagram – Master Thesis	80

List of Tables

5.1	Multiphase booster limitations	35
5.2	Visualization equipment	36
5.3	Camera and light settings	36
5.4	Main Instruments	37
5.5	Experimental test matrix	40
6.1	Maximum pressure oscillation at surging relative to the re- spective average pressure	58

Chapter 1

Introduction

This chapter will introduce the background and motivation of the work performed. Challenges and limitations during the project will also be stated here. In addition, this chapter will present the thesis scope, and give an overview of the report structure.

1.1 Background

Multiphase pumps are one of various techniques used for increasing oil and gas recovery, and the petroleum industry has started to apply the technology on a larger scale. The technology is expected to improve production of gas rich fields, by replacing the needs of separating the gas from the oil, and consequently, compress the gas and pump the liquid separately. Multiphase pumping is defined as the boosting of liquid composed by gas contents between 10% and 95%. For higher gas fraction flows, wet gas compressor systems are utilized.

Multiphase boosting improves the production economics by reducing the backpressure of the reservoir which increases the flow rate. The technology has been applied in production extension of ageing and low energy reservoirs. In addition, subsea multiphase pumps permit an extended tie-back distance between the well and the host by adding pressure to the flow. This make it possible to have a central processing facility hosting multiple wells at the same time. During the last years, research has resulted in improvements of the technology. Snøhvit and Ormen Lange are two operating fields employing the multiphase boosting in terms of "subsea to beach" (eliminating platform). Such subsea production stations are desirable in order to reduce personnel risks and operation costs offshore. Multiphase pumping is also a beneficial method both economical and environmental, due to reduction of

the gas flaring compared to conventional separation and compression methods [21]. More information about the fields of application, subsea, offshore, and onshore are reported in [16].

Two-phase pumps are divided into two main categories, rotodynamic (helico-axial and electrical submersible pumps (ESP)) and positive displacement (twin screw pumps) concepts. The choice depends on the compromise between the desired flow rate and the head, as well as the operating range. Rotodynamic pumps have a higher volumetric capacity compared to the positive displacement pumps. Kinetic energy is added to the fluid by the impeller; the energy is thereafter converted into static pressure energy by decelerating the flow velocity in the diffuser. Throughout this energy conversion, the flow will have a high risk to separate, which will reduce the machine performance. Positive displacement pumps are however not so sensitive to phase separation, where a fixed amount of the fluid is trapped and forced to a higher static pressure level. This thesis focuses on a mixed-flow single stage rotodynamic pump, which reproduces the multistage pump, "Multi-Booster", designed for a wide gas handling capability up to 90% gas volume fraction (GVF) in continuous operation. The impeller is specifically meant to provide a well mixed flow with low phase slip.

A safe operation is important to avoid machine breakdown and damage of components downstream. Instability and surging provide a discontinuous flow field, and are important issues in multiphase boosters. Moreover, operating failure is critical due to reduction or total stop of the production from the machine. The multiphase flow characteristics depend strongly on the gas volume fraction (GVF), flow rate, flow pattern, inlet pressure, and rotational speed. Subsea installations, in particular, should be even more resistant to the unwanted conditions, due to inaccessibility. A fundamental understanding of how the complex flow phenomena and transients affect the machine operation, and is essential to obtain a reliable and efficient pump design.

1.2 Challenges

Due to the complex nature of multiphase mechanisms, more knowledge is here necessary in order to understand the fluid dynamic and thermodynamic behavior in the multiphase booster.

The pump shows to be sensitive in terms of flow transients, such as changing flow patterns. The current lack of existent analytical or empirical two-phase models introduces a challenge in order to verify the experimental results.

1.3 Scope of Thesis

This thesis explores the surging inception and evolution through an extensive test campaign in cooperation with the PhD project "MultiBooster Performance". Direct flow visualization with a high-speed camera combined with a data processing system (NI DIAdem) have been utilized in order to relate the pressure pulsations to two-phase flow mechanisms during the unstable machine operation. Characteristic flow phenomena are detected and will be analyzed through flow visualization and data processing.

A literature review has been performed in order to document previous approaches to define surging in multiphase pumps. Additionally, a literature review considering phase slip and related physical mechanisms in a rotodynamic pump, has been conducted in order to assess a deeper understanding of the flow field behavior. Bubble tracking and bubble behavior analysis are performed.

A broad data collection has been acquired in correspondence with the test campaign considering the unsteady machine operation. Furthermore, a detection method of the surging inception has been presented with respect to the correlation between GVF and discharge pressure pulsations.

1.4 Limitations

Documenting phase slip in the multiphase booster has shown to be a challenging task and would require an extensive test campaign. The assessment and documentation of phase slip and bubble behavior were planned to be performed through an advanced bubble tracking software. After several attempts and request from professional help, the tracking tool showed to be limited for this type of application because of the high flow complexities. Additionally, an extensive literature review shows a very restricted information regarding phase slip correlations compatible with the multiphase booster.

The current visualization technique shows limitations when considering flow field characterized of by high disturbances. More advanced visualization and measurement techniques are required to give a more complete understanding of the two-phase mechanisms (e.g. laser Doppler Velocimetry (LDV) or Particle Image Velocimetry (PIV)).

1.5 Report Structure

The thesis main contents are listed below:

- **Chapter 2:** Gives an overview of fundamental pump theory, multi-phase definitions, and two-phase modeling. In addition, this chapter presents and discusses relevant two-phase flow pattern.
- **Chapter 3:** Reports observations from literature reviewing phase slip and other related mechanisms. Characteristic bubble behavior observed from visualization will be discussed. Available phase slip correlations and an evaluation of image-based metrology will also be presented here.
- **Chapter 4:** Describes previous investigations from an extensive literature review considering multiphase pumping instabilities and surging.
- **Chapter 5:** Presents the test facility and the experimental method.
- **Chapter 6:** Presents and discusses the main investigations from the experiments conducted. The chapter presents and discusses the most important observations regarding flow phenomena during surging inception and evolution. Furthermore, a surging inception detection method is presented here.
- **Chapter 7:** Gives a conclusion from the previous chapters.
- **Chapter 8:** Proposes suggestions for future work.

Chapter 2

Fundamental Theory

Multiphase booster operation is dependent on the multiphase fluid parameters, as well as the hydraulic pump design. The first part of the chapter gives a brief introduction of pump theory with regards to single phase operation, which is essential to understand the physical mechanisms in the multiphase booster. The presence of gas affects both performance and system stability. Consequently, the next part gives a brief overview of two-phase performance modeling, and relevant theoretical multiphase definitions and flow patterns will also be presented here.

2.1 Pump Theory

The single phase pump theory is outside the thesis scope, and will therefore be covered briefly. As mentioned in the introduction, the purpose of the pump is to deliver steady flow and a certain pressure. In a rotodynamic pump, fluid is accelerated in the impeller, before the flow is decelerated in the diffuser, where energy is converted into static pressure energy.

In single phase pumps, the ideal impeller energy transfer can be derived through an impeller momentum balance considering the inlet and outlet flow conditions. After necessary assumptions and pre-calculations [25], the theoretical head at nominal operation is given by the Eulerian head equation.

The equation is given by:

$$H_{th} = \frac{V_{2u}U_2 - V_{1u}U_1}{g} \quad (2.1)$$

In addition, pumps are commonly designed due to the principle of no inlet swirl. This leads to zero inlet circumferential velocity component:

$$V_{1u} = 0 \quad (2.2)$$

thus,

$$V_1 = V_{1m} \quad (2.3)$$

Hence, the equation (2.1) can be written as:

$$H_{th} = \frac{U_2 V_{2u}}{g} \quad (2.4)$$

The pump category depends on the impeller shape, where the most common ones are axial, semi-axial and radial. A semi-axial impeller design is favourable due to the centrifugal and Coriolis acceleration have opposing components [25]. This is meant to reduce the risk of flow separation and provide an improved phase mixing.

The semi-axial impeller design is characterized between the axial and radial design. In operation it provides less head compared to a radial impeller, but can handle higher flow rates. This relation is the opposite compared to the axial impeller design. Lea and Bearden [26] reported that mixed-flow impellers were able to handle gaseous fluids better than the radial, due to the improved capability of avoiding gas pockets and total blockage (gas-locking).

Figure 2.1 shows a simplified semi-axial blade sketching from circumferential and meridional view perspective.

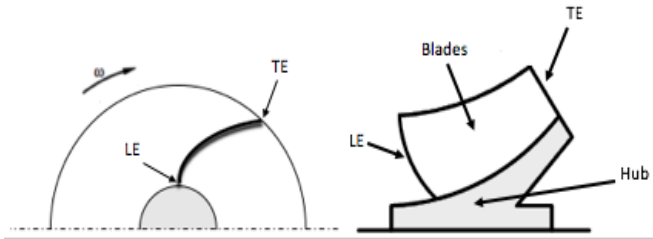


Figure 2.1: Circumferential and meridional view of a semi-axial impeller

Furthermore, the inlet and outlet impeller velocity triangles are illustrated in Figure 2.2.

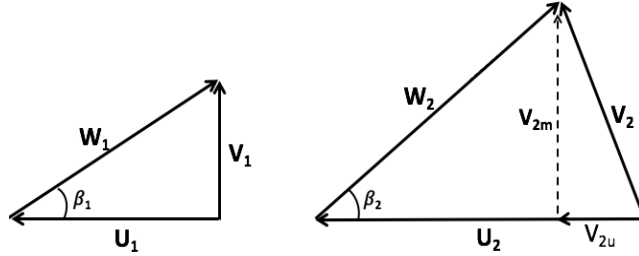


Figure 2.2: Velocity triangles inlet (left) and outlet (right)

This thesis considers two-phase operation at partload. Consequently, this condition is characterized by the deviation between flow and blade angle causing additional losses due to incidence and recirculation.

Sachdeva [39] lists the different losses affecting the ideal single phase pump performance into five groups:

- Incident losses and slip losses
- Mechanical: losses in bearings and shaft seals, also termed as external losses [25]
- Leakage: volumetric losses through the clearance between the rotating and static components
- Disk friction: energy dissipated as a consequence of the material friction
- Hydraulic: friction, flow separation and turbulent dissipation losses due to changes in the flow direction and velocity

The losses are found further explained by Gülich [25].

It should be noted that two-phase flow operation enables completely different mechanisms. However, the losses are relevant for particular two-phase models considering pump operation at very low gas contents, where a quasi single phase flow is assumed.

2.2 Multiphase flow

Multiphase flow is defined as a simultaneous occurrence of more than one phase. Water and air, respectively, will be considered as the continuous and dispersed phase throughout this thesis. The phases will have the subscripts l and g , respectively. Multiphase flow in real operation will typically contain oil, gas and sand.

Multiphase boosting is of interest to the oil and gas industry due to beneficial production and costs, but introduces several challenges due to complex physics involved. Pumps utilized in the process industry should be tolerant to a wide spectre of flows, and be reliable in order to assure a steady and suitable flow to the components downstream.

2.2.1 Two-Phase Fundamentals

As identified, the multiphase characteristics influence the pump performance and stability. Some of the most important multiphase flow definitions used the literature are listed below. The gas volume fraction (GVF) and gas mass fraction (GMF) indicate the flow composition, expressed through equation (2.5) and (2.6).

Gas Volume Fraction (GVF):

$$GVF = \frac{q_g}{q_g + q_l} \quad (2.5)$$

Gas Mass Fraction (GMF):

$$GMF = \frac{\dot{m}_g}{\dot{m}_g + \dot{m}_l} = \frac{\rho_g GVF}{\rho_g GVF + (1 - GVF)\rho_l} \quad (2.6)$$

The total volumetric flow rate is vital in pump performance calculations.

Total volumetric flow rate is defined as:

$$q_{tot} = q_l + q_g \quad (2.7)$$

According to the gas compressibility, the volumetric gas flow will reduce within the multiphase booster, leading to a decreased GVF. The total mass flow through the pump will however remain constant.

Total mass flow rate:

$$\dot{m}_{tot} = \dot{m}_l + \dot{m}_g = \rho_l q_l + \rho_g q_g \quad (2.8)$$

The superficial velocity denotes the velocity each phase would have had if this was the only one present in the cross-sectional area [40]:

Superficial velocity, gas:

$$V_{s,g} = \frac{q_g}{A_{tot}} \quad (2.9)$$

Superficial velocity, liquid:

$$V_{s,l} = \frac{q_l}{A_{tot}} \quad (2.10)$$

When assuming no slip, the following relations between the actual and superficial velocities can be applied:

$$V_g = \frac{V_{s,g}}{GVF} \quad (2.11)$$

$$V_l = \frac{V_{s,l}}{(1 - GVF)} \quad (2.12)$$

The phase slip velocity represents the relative phase velocity. This parameter is of particular importance when considering segregated flows.

Relative phase velocity:

$$V_r = |V_l - V_g| \quad (2.13)$$

The phase slip is often denoted through the slip ratio:

$$\gamma = \frac{V_g}{V_l} \quad (2.14)$$

Homogeneous flow assumes no phase slip ($\gamma = 1$).

The void fraction (VF) plays a key role in determining other important parameters, such as the two-phase density and the relative phase velocity. It is also of fundamental importance in two-phase prediction models.

Void fraction:

$$VF = \frac{A_g}{A_g + A_l} \quad (2.15)$$

The parameter is most widely defined as the cross-sectional, where A_g and A_l are the cross-sectional areas occupied by vapor and liquid, respectively. The void fraction can also be specified by other geometrical expressions; local, chordal and volumetric.

The density ratio, ρ^* , indicates the level of phase interaction and phase separation.

The density ratio is given by:

$$\rho^* = \frac{\rho_g}{\rho_l} \quad (2.16)$$

A high density ratio indicates a high risk of phase separation. This parameter is also dependent on the gas compressibility.

The reason for defining the gas mass fraction, slip ratio, and the void fraction is because some two-phase models require these values in order to calculate the two-phase mixture density, which are further used to calculate the pressure drop.

2.2.2 Two-phase Modeling

Predicting and analyzing the flow behavior are important issues in multiphase flows. Multiphase pump performance is outside the scope, but will be briefly documented due to the influence of the two-phase instabilities, studied later in this thesis, have shown to influence the pressure production across the pump, which affects the performance.

Homogeneous flow model:

The two-phase models neglect the relative motion between the phases by assuming a homogeneous mixture. Consequently, the model is applicable to flows characterized by fine dispersed bubbles entrained in the continuous phase causing no relative motion. Furthermore, the fluid is treated with a mixture density as a function of each of the phase densities.

The mixture density is given by:

$$\rho_{hom} = \rho_g GVF + \rho_l (1 - GVF) \quad (2.17)$$

The homogeneous flow model can in some cases give satisfactory approximations for bubbly flows and mist flows. Consequently, the model is not valid for irregular flow conditions, such as surging.

Two-fluid models:

At significant GVFs, the flow can no longer be assumed as a homogeneous mixture. The two-fluid models treat each of the phases as separated with equations dedicated to the specific phase. Conservation equations due to mass, momentum and energy are developed for the two-fluid flows including the respective interaction terms between the two flows. Further information about two-fluid models can be found in [7, 32].

Computational fluid dynamics (CFD):

Computational methods are applied in numerical analysis providing a detailed description of the flow. The tool is frequently used by the industry for various engineering applications due to design and prediction purposes. CFD includes multiphase flow models with regards to simulation of multiple fluid streams, bubbles, droplets, free surface flows and solid particles. There are two main multiphase flow models; Lagrangian Particle Tracking model and Eulerian–Eulerian model [14]. Barrios and Prado used the latter model in a study investigating the onset of surging in a ESP.

Multiphase flow phenomena require a very fine discretization, both with regards to temporal (time-step) and spatial (grid), due to the physical complexity. It should be noted that successful computations utilizing CFD require a complete understanding of the flow physics. At some distant time, the computer may be able to solve the Navier-Stokes equations for each of the phases and to compute every detail. However, this would require a certain improvement of the computer capacity.

Impeller body forces and gravitational forces affect the phases differently due to their fluid properties, making it difficult to obtain a mathematical description of the flow. Two-phase models are explored through different methodologies; experimentally, theoretically, and computationally. Furthermore, available models show to be convenient for conditions close to the design point for low GVFs, but give inaccurate predictions with respect to partload operation.

More details regarding two-phase flow models can be found in [7] by Brennen.

2.2.3 Flow Pattern

This thesis explores the flow pattern during unsteady machine operation to improve the understanding of two-phase flow behavior. By analyzing the specific flow pattern, is expected to be of great value in order to explain flow field trends.

In general, a method to define the different flow patterns, is to create flow pattern maps based on experimental investigations. The superficial velocity of liquid and gas are often used to plot the flow pattern maps. A flow pattern transition is recognized when a flow pattern becomes unstable and forms into another one. This can be associated with the transition between laminar and turbulent flow regimes.

The multiphase booster capability is strongly dependent on whether the gas and liquid form a homogeneous mixture or separate from each other. High values of phase slip indicate higher risks of phase separation, affecting both the booster performance and system stability. For low GVFs, the bubbles are entrained in the continuous phase, but for larger gas flows bubbles accumu-

late into larger zones hindering smooth pump operation. Further increasing the GVF will eventually lead to gas-locking.

Figure 2.3, depicts a flow pattern map for two-phase flow patterns in a horizontal pipe.

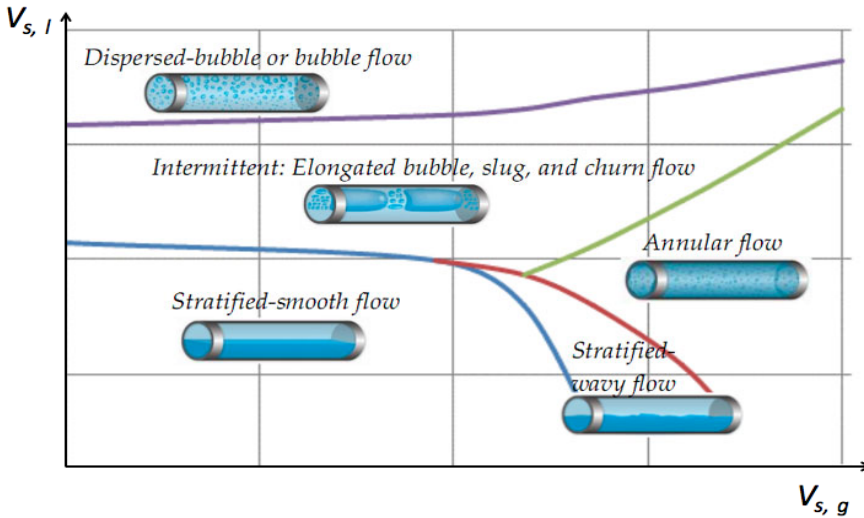


Figure 2.3: Flow pattern map in a horizontal pipe, [36]

Figure 2.3 shows that stratified flow occurs due to low superficial gas and liquid velocities, dominated by gravity and buoyancy forces. In the other end, annular flow pattern is predicted, characterized by high superficial gas velocity and low superficial liquid velocity. Furthermore, the transition from bubble flow to elongated and slug flow occur with decreasing superficial liquid velocity. Figure 2.4 shows the separated and dispersed two-phase flow pattern in a horizontal pipe.

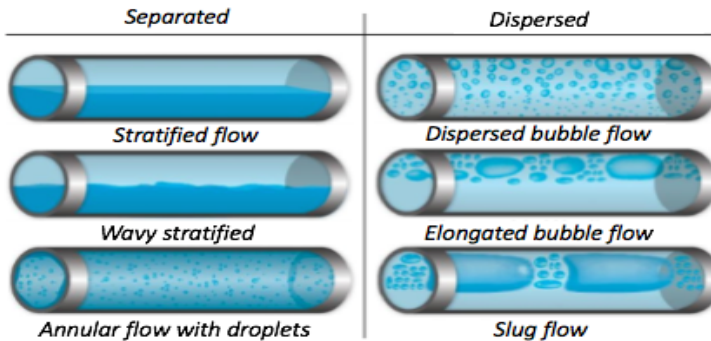


Figure 2.4: Flow regimes in a horizontal pipe [36]

In general, visual observations during partload operation reveal several flow regimes represented in Figure 2.3 and 2.4. The flow patterns of main importance during are outlined below.

Dispersed Flow

Bubbly flow is characterized by small individual gas bubbles distributed uniformly entrained in the liquid continuous phase. This flow pattern indicates a high drag, and is therefore desired due to low risk of phase separation. The increase of liquid flow rate results in a higher turbulence level, which further indicates smaller bubbles and improved phase mixing. In cases with either increasing the GVF or reducing the flow rate, induce flow transitions characterized by bubble coalescence forming into larger gas accumulations obstructing the channels.

In addition, the flow pattern goes from fine bubbles towards elongated bubble flow or slug flow. The low density phase appears as large bullet shaped bubbles (more distinctive in slug flow than elongated bubble flow) separated by liquid bulks. These flow regimes affect the pump with higher stresses and vibrations causing system instabilities. Such flows can be observed at the pump inlet and within the blade channels when approaching the surging zone. Gas pockets affect the pump operation by blocking parts of the channels, indicated by the reduced delivery pressure. Further increasing the GVF will eventually lead to gas-locking causing zero pressure increase across the pump.

Separated Flow

Figure 2.4 shows three types of separated flow; (1) stratified, (2) wavy stratified, (3) and annular flow. The three flow pattern are all characterized by relatively low superficial liquid velocity, and increasing superficial gas velocity with respect to the flow pattern numbering.

During unstable machine operation, flow separation and flow pattern transitions have been observed by flow visualization. The transition from wavy stratified to annular flow is recognized as the transition from surging onset to gas-locking. The latter condition occurs at flows characterized by high GVFs obstructing the incoming flow. Furthermore, the annular flow is recognized by the high density phase (water) acting as droplets in the continuous low density phase (air). The radial pressure gradient is here forcing the high density phase towards the annulus. Consequently, the liquid appears adhered to the pleixi, observed as a wavy film moving slightly forward.

2.3 Summary

Relevant multiphase flow transitions during unsteady machine operation have been presented. The multiphase flow pattern characteristics are in-

fluenced by several factors; flow rate, GVF, pump design, gravitational and body forces. With the increase of GVF, the flow pattern, as well as the differential pressure across the pump changes dramatically as a consequence of the increased channel obstructions. Flow transitions have been observed; (1) bubbly flow towards elongated flow or slug flow when approaching surging, (2) and wavy stratified towards annular flow during surging. Observations with regards to specific flow phenomena and trends will be discussed in Chapter 3 and 6.

Chapter 3

Visual Flow Analysis

Adding gas to the liquid flow will introduce operating challenges to the pump, affecting both the performance and booster system stability. The phase slip denotes the relative phase behavior between the gas and liquid, often described through the slip ratio (γ) and superficial phase velocity. However, the flow analysis inside a rotating channel is a fundamental issue for many engineering applications, leading to the necessity of major assumptions. Several studies reported in literature dealing with this topic, often neglect the effect of phase slip due to the high complexity. High phase slip increases the risk of phase separation, where the associated mechanisms should be studied in order to avoid unsteady machine operation.

This chapter includes a literature review concerning phase slip and the related physical mechanisms. Fundamental body forces and transversal fields acting in a rotating channel will be presented. The phase slip is expected to be a highly complex phenomenon, dependent on various influencing effects. This chapter aims to narrow down the problem, and focus on the bubble behavior in particular. Consequently, observations from bubble analysis will be presented in this chapter. In addition, phase slip will be discussed in terms of available correlations and visualization.

3.1 Associated Phase Slip Mechanisms

The pump capability to transport the multiphase flow depends in the first place on whether gas and liquid form a homogeneous mixture or to what extent the two phases separate [25]. A homogeneous mixture, such as in bubbly flow where fine bubbles are entrained in the continuous phase, can be characterized as quasi single phase flow. The phase slip is often reported to be neglected, which shows to be feasible for very low gas fraction flows, but becomes inaccurate with the increase of GVF. The phase slip is expected

to lead to phase separation, which is assumed to be one of the main problems in a rotodynamic pump [40].

3.1.1 Rotating Channel Flow

In order to understand the flow behavior inside the pump, it is important to have knowledge about the main influencing forces. The impeller generates body forces, acting differently on each of the phases dependent on its properties (density and viscosity). The flow field irregularities are difficult to analyze, which further make computational analysis (CFD) a comprehensive task.

Murakami and Minemura et al. [27, 28, 33] investigated the bubble characteristics and flow patterns in centrifugal pumps under different operating conditions. They observed four different flow patterns; segregated gas flow, gas pocket flow, bubbly flow and isolated bubble flow. The bubbles showed to move slower than the surrounding liquid along the impeller pressure gradient. Furthermore, the effect of phase slip and the pressure gradient were found to be the main influencing factors on the bubble motion [27]. The phase slip was established due to velocity difference between the liquid and gas phase.

The pump rotational speed affects the bubble behavior. Li and Xue [38] proposed phase separation to be dependent on the rotational speed as well as the curvature radius of the impeller. Zhang et al. [22] studied the two-phase flow inside a rotodynamic multiphase pump and concluded that the bubble size decreases with the increase of rotational speed, accordingly. This conclusion was based on two main aspects: (1) Increased drag force of liquid to gas due to higher slip velocity. (2) The increasing liquid turbulence level causes larger bubbles to split into smaller ones. In addition, the increased turbulence level forces larger bubbles to break due to improved phase mixing. Furthermore, they observed an increasing average bubble size with the increased gas fraction, when maintaining the rotational speed and flow rate constant.

The variations in the phase velocity, induced by the impeller, causes a higher risk of phase separation. Furthermore, Zhang et al. [22] analyzed the forces acting on an isolated bubble. The analysis was performed in order to determine the location of gas pockets in the flow. The analysis bases on the following assumptions [22]:

- Two-phase mixture thermodynamical equilibrium
- Zero mass transfer
- Constant temperature regardless of the surrounding fluid interaction and the interaction force between bubbles

The bubbles are mainly subject to the drag force, centrifugal, Coriolis forces, gravity and buoyancy forces, as well as the pressure gradient in the flow direction and the vertical flow direction [22]. The main influencing forces on an isolated bubble are illustrated in Figure 3.1.

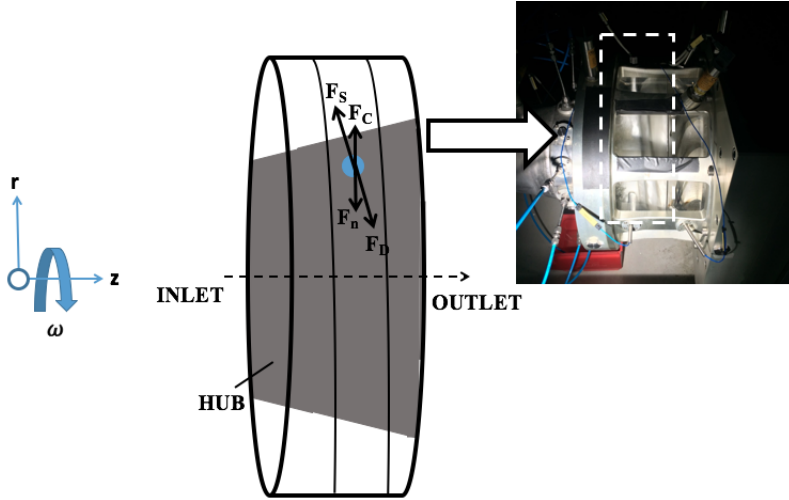


Figure 3.1: Main influencing forces on an isolated bubble

where,

- F_D : Drag force on the bubble by the surrounding continuous phase
- F_C : Centrifugal force on the bubble pointing outward along the impeller radius
- F_n : Pressure gradient in the radial velocity direction
- F_S : Pressure gradient in the relative velocity direction

The flow is also the Coriolis acceleration, acting perpendicularly to the relative velocity direction (assumed to follow the channel axis) [25]. Furthermore, the semi-axial impeller designed to provide a balance between the centrifugal and Coriolis forces, making them act in the opposite directions. Measurements of the forces depicted in Figure 3.1 is outside the thesis scope and will not be performed due to missing measurement techniques. However, this would be of great value in order to understand their influence on the flow field. Some of the effects identified above will be discussed later in this chapter.

3.1.2 Transversal Acceleration Field

Based on flow visualization, the multiphase booster flow field is characterized by transversal acceleration fields. This mechanism is expected to affect the risk of phase separation, involving a change in the phase slip and, consequently, the pressure evolution across the pump.

Bratu [5] developed an analytical two-phase flow model considering the pressure rise and void fraction evolution in a rotodynamic pump. The model is expected to give valuable results due to this application assumed the required measurement and visualization tools were available. The model and the according equations are explained in detail in [5].

Transverse motion can be obtained with analytical models including the continuity, momentum, and energy equations. The numerical integration refers to the solution of the Navier-Stokes equations. Additionally, such calculations can also be performed in terms of numerical integration methods as Runge-Kutta [37, 8], or by analytical approximations. The feature is dependent on the local pressure gradients, void fraction, the body forces (centrifugal and Coriolis) as well as the drag force [5]. However, calculations would require local measurements regarding fluid properties, phase velocities and flow angles.

Based on the studies from available literature, the effect of transversal acceleration fields appear as a very complex phenomenon to analyze. Other features are assumed to be more important, and should be prioritized in order to document the phase slip.

3.1.3 Bubble Behavior

Several studies are based on major assumptions such as neglecting the bubble effect on the pressure field and the liquid phase velocity. By studying the bubble behavior, it is believed to improve the understanding of the physical mechanisms in the two-phase flow.

High-speed videos permit a detailed view of bubbles in the complex flow field. Bubbles are observed in various shapes and sizes. Also, the bubble behavior is observed to change along the flow path. The influencing forces are mainly caused by the impeller, illustrated in Figure 3.1. Other minor influencing forces, are the effects of bubble viscosity and density. An extensive review of models and measurement techniques for two-phase flow in straight channels can be found of the research by Clift et al. [15], and Jakobsen [23].

In terms of bubble behavior analysis, one should have fundamental knowledge about bubble shape properties. Clift et al. [15] reports a bubble regime map in "Bubbles, Drops, and Particles", applied for bubble shape prediction with respect to the Eötvös and Reynolds numbers. The dimensionless

numbers; Weber, Eötvös, Morton and Reynolds play a key role in the study of bubble shape and bubble motion.

The parameters are defined as:

(1)

Eötvös number – ratio between gravitational and surface tension forces:

$$Eo = \frac{g\Delta\rho d_p^2}{\sigma} = \frac{\textit{inertial force}}{\textit{surface tension force}} \quad (3.1)$$

(2)

Morton number – involving the pressure field and physical properties of the surrounding liquid:

$$Mo = \frac{g\mu^4\Delta p}{\rho_l^2\sigma^3} = \frac{(\textit{viscous force})^4 (\textit{buoyancy force})}{(\textit{inertial force})^2 (\textit{surface tension force})} \quad (3.2)$$

(3)

Reynolds number for a particle – ratio between inertia- and the viscous forces:

$$Re_p = \frac{\rho_l d_p V_r}{\mu_l} = \frac{\textit{inertial force}}{\textit{viscous force}} \quad (3.3)$$

(4)

Weber number determining the ratio between inertia- and surface tension forces:

$$We = \frac{\rho_l V_r^2 d_p}{\sigma} = \frac{\textit{inertial force}}{\textit{surface tension force}} \quad (3.4)$$

(5)

In addition, the modified Fronde number [5] was employed in the two-phase model developed to determine the extent of flow separation in a rotodynamic pump. The modified Fronde number is given by the following definition:

$$Fr = \frac{\rho_g V_g^2}{T [C - R - B]} \quad (3.5)$$

where:

T: gas layer thickness

C: Coriolis acceleration

R: centrifugal acceleration

B: acceleration due to the radius of the curvature of impeller blade

The Weber number is selected as a criterion judging the stability of an isolated bubble when evaluating the dispersion and bubble coalescence in a

rotating impeller channel [10]. Furthermore, the Weber number is used for describing the stability of droplets in gas flows, associated with the annular flow regime during pump gas-locking. Figure 3.2 pictures a map containing generalized bubble regimes in terms of the Eötvös and Reynolds numbers. This is used for estimating terminal velocity as well as to determine the bubbles and liquid drops shape regimes in an unhindered gravitational flow.

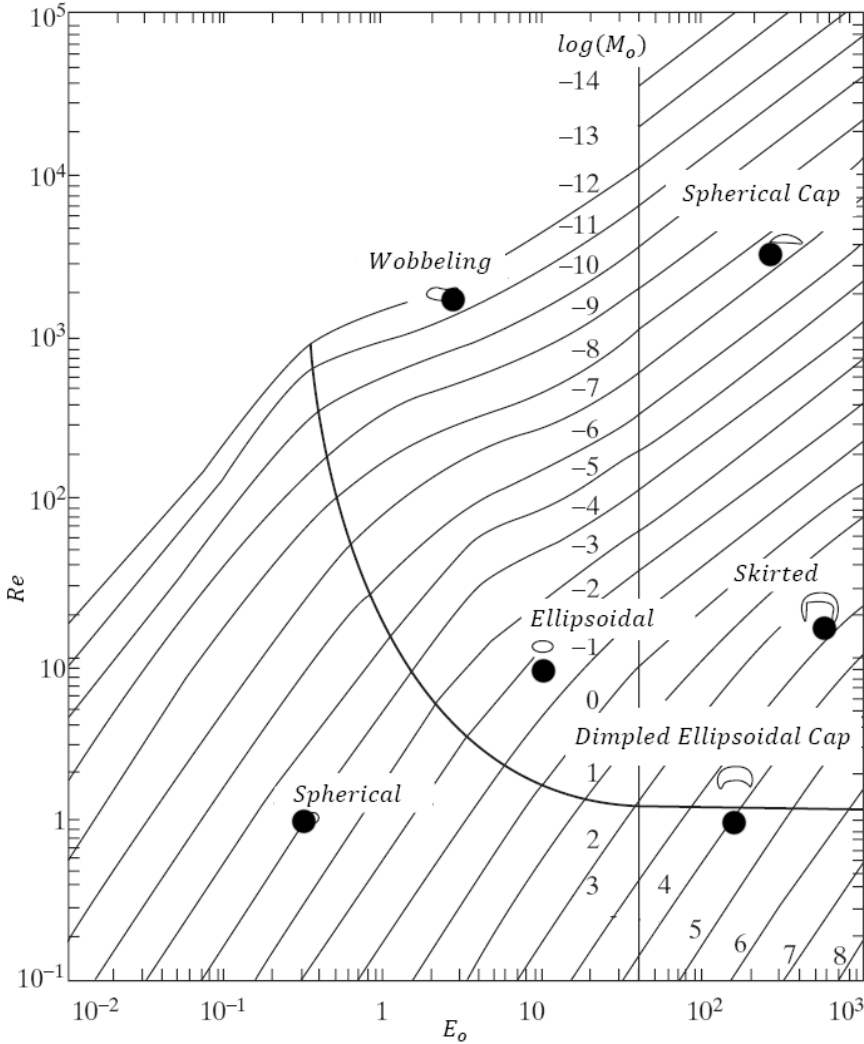


Figure 3.2: Bubble shape regimes and transitions [15]

The map gives a brief overall view of various bubble shape regime transitions. In addition, it demonstrates the wide range of bubble and drop behaviour

[42]. The bubbles tend to deform when they are influenced by asymmetric forces, such as those in the rotating channel. Based on flow visualization the majority of the bubbles has an irregular shape, close to the wobbling regime seen in Figure 3.2.

Experimental work shows the bubble shape to be maintained by the balance between the shear force, normal force, surface tension force, as well as the buoyancy. In this thesis experiments, the bubbles are influenced by rotating effects and phase interaction which make flow visualization very challenging. The inlet flow field, however, contains less disturbances at low rotational speeds due to low influencing body forces from the impeller. Figure 3.3 shows a bubble trajectory approaching the channel inlet under the following condition: 900 rpm and 70% q^* , at the onset of surging.

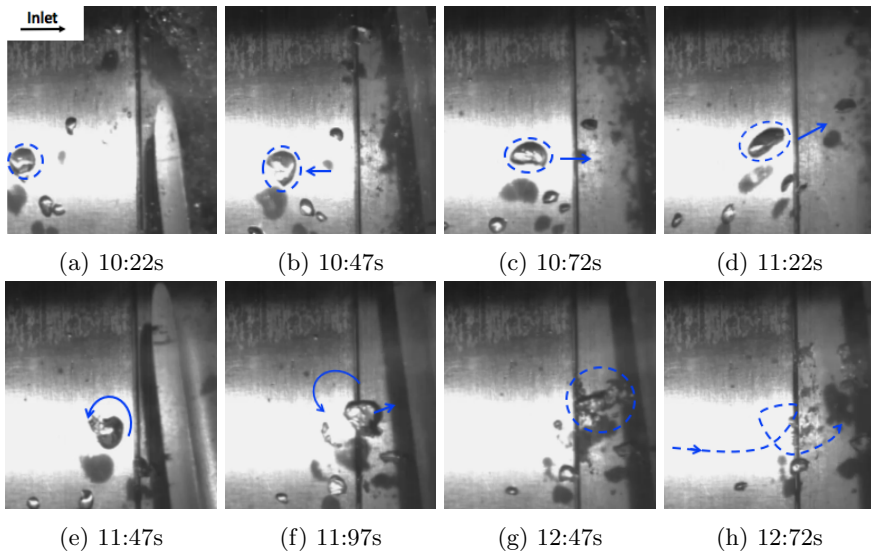


Figure 3.3: Bubble trajectory at 900 rpm and 70 % q^*

The inlet flow field condition is recorded with a camera fps of 500 Hz and analyzed with a playback speed of 0.01 relative to the original play speed. This makes it possible to analyze the bubble motion and shape approaching the impeller inlet. In Figure 3.3a a selected bubble, indicated with dashed blue circle, is observed to have a quasi spherical shape. Thus, the bubble surface tension is in balance with the external forces. The bubble is forced towards the pump inlet by the drag force of the liquid phase and sucked into the impeller. As a consequence of the unstable surging condition, the bubble motion is affected by a consecutive deceleration and acceleration, consequently. The flow field fluctuations deform the spherical bubble shape, as can be seen in Figure 3.3b and 3.3c. Furthermore, the pressure gradient caused by the impeller is indicated by the "bubble nasal" (bubble front tip) pointing in the respective direction (seen in Figure 3.3d). The following

blade rotation creates a transverse pressure gradient causing a 360° counter clockwise rotation, before the drag force leads it towards the blade suction side, where it breaks into small bubbles. Figure 3.3h summarizes the trajectory covered by the bubble.

The current visualization technique allows successful bubble tracking, consequently, the bubble motion and shape, for particular operating conditions. Principally, the capturing shows to be feasible at the inlet section, where the influence of body forces is low compared to inside the impeller channels where bubble trajectory appear close to impossible due to the visual limitations. An extensive test campaign should be performed in order to document the influencing forces more into detail. Furthermore, the bubble behavior analysis is of further interest with regards to improve the accuracy of computational algorithms and two-phase models.

3.2 Available Phase Slip Correlations

Phase slip correlations have been studied through a literature review. The main intention is here to assess a fundamental knowledge in order to document phase slip trends observed by flow visualization. Also, the phenomenon is reported to affect the hydraulic head (pressure) and should therefore be fully understood to avoid unwanted operating regimes.

In agreement with Ole Jørgen Nydal professor in multiphase pipe flow at NTNU and the thesis main supervisor, documenting phase slip in a multiphase pump is highly complex. Thus makes difficult to obtain relevant information on the specific topic.

Two-phase models are often formulated as an extension of the single phase theory. Typically, the phase slip is of interest in order to predict the two-phase pump performance. Based on the literature review, the two-phase models often based on several two-phase simplifications, such as spherical bubbles and homogeneous mixture. The latter assumes no phase slip, which is the case for the majority of the empirical performance correlations published [40]. Consequently, this might give useful results for specific conditions with very low gas content, but becomes inaccurate for flow pattern transitions and during elongated bubble flow [24].

Figure 3.4 shows a comparison between the pressure increase calculated with the homogeneous model versus the experimental results for elongated flow, reprinted from [24].

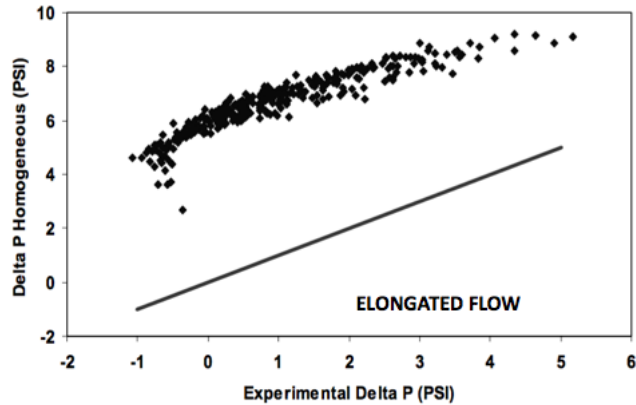


Figure 3.4: Experimental pressure increment for elongated flow versus homogeneous pressure prediction [24]

The difference between the experimental results show a substantial deviation from the analytical prediction. This indicates that the two phases are no longer flowing in agreement with the laws of physics applicable to single phase flow. A satisfactory pressure prediction would require corrections of the homogeneous two-phase model.

The presence of gas is expected to induce phase slip, which will affect the pressure production accordingly. Bratu [5] used the conservation equations of mass and momentum for two-phase flow to obtain the changes in void fraction to estimate the correlated slip ratio. Higher phase slip corresponds with an increasing gas void fraction and bubble coalescence causing flow field irregularities. Furthermore, the obstructions cause strong pressure fluctuations and relative phase accelerations, causing unsteady delivery flow to the components downstream.

Flow visualization indicates the motion of the phases to be dependent on the flow pattern. Thus, the phase slip behavior varies with the flow pattern. This causes a real challenge during surging, where the flow pattern changes frequently. Also, the void fraction variation and separation effects become significant when operating at higher gas flow rates.

The field of research has shown to be in an early stage for this type of application. A complete understanding of the phase slip mechanisms would be of great value to improve the prediction of two-phase pump performance and reduce the risk of flow separation. An extensive test campaign should be conducted, accompanied with computational simulations and advanced visualization and measurement techniques. It should be noted that a fea-

sible model would be restricted to the specific pump size and geometry, superficial phase velocity, fluid properties, as well as the flow rate and rotational speed.

3.3 Evaluation of Image-Based Metrology

Image-based metrology is intended to explore phase slip trends in the multi-phase booster. The visualization technique used is further described in Section 5.2. The visualization method, high-speed camera by PFV (Photron FASTCAM Viewer), is able to acquire images with 6000 fps (frames per second). In addition, the videos have been employed in order to analyze the bubble behavior. A more advanced bubble tracking tool, also by PVF (Photron FASTCAM Analysis), expected to give a detailed bubble analysis has also been evaluated here.

Various combinations of image size (pixels), exposure time (shutter speed) and fps (images per second) have been conducted in order to obtain the most suitable view. The rotating effects from the impeller make it difficult to observe isolated bubbles within the hydraulic channels (see Figure 3.5). However, a step in the right direction is to start from simple cases considering the section with relatively low disturbances, such as the impeller inlet as done in Figure 3.3, showing a successful bubble trajectory.

Among other disturbances, the varying reflections from the bubble and hub background, bubble wobbling, and clusters (touching bubbles) make the bubble tracking to a challenging task. Simplifications are here necessary, and should be considered in further work. Algorithms to avoid image aliasing, bubble image processing and illumination compensation [11, 12, 20] could be of great value for this application. The algorithms are applicable for low void fractions in straight channel flows. These regimes represent a simplified condition compared to this application, but may be applicable to the pump inlet region, where body forces are not so strong. Partload operation provides high flow irregularities governed by complex mechanisms. Additionally, the high bubble velocity and phase interaction make it difficult to track a single bubble over a certain period of time.

The progressively increasing flow field complexity is shown of the succession of images in Figure 3.5. The images indicate the flow field when approaching the onset of surging (left to right). The upper and lower row show the impeller channel and diffuser channel, respectively.

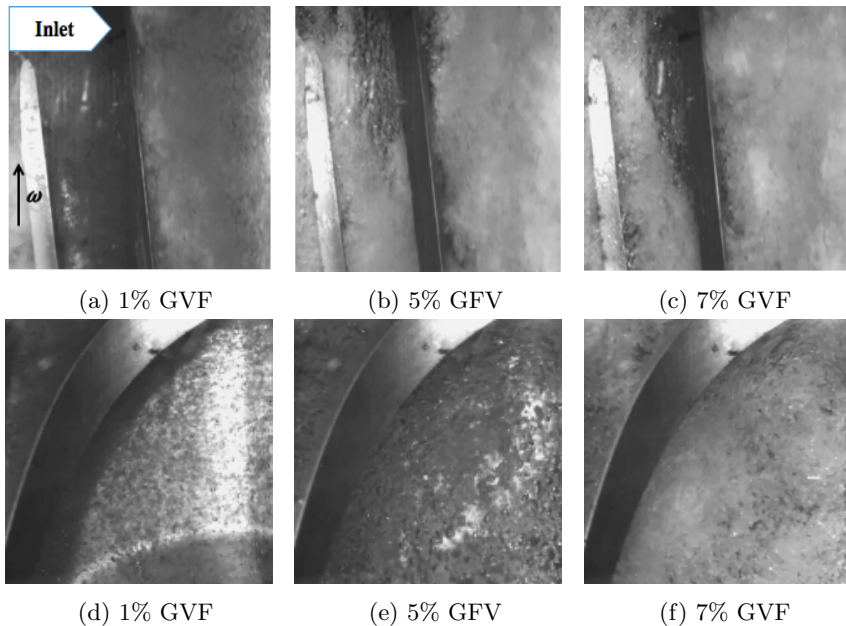


Figure 3.5: Flow visualization – rotating channel (upper row) and diffuser (bottom row) at different GVFs, 1200 rpm and 50% q^*

Figure 3.5a and 3.5d show the flow field at 1% GVF. The flow is characterized by fine dispersed bubbles indicating a quasi homogeneous mixture with low phase slip. Increasing GVF results in a more crowded flow pattern. The bubbles are closely gathered, appearing as white foam. An annular flow pattern region is observed in Figure 3.5b indicated by a liquid film adhered to the transparent casing, indicating high gas obstructions inside the channel. Consequently, this leads to relative phase velocity and thus a higher phase slip. The size and number of the bubbles are seen to increase in the diffuser channel when comparing Figure 3.5d to 3.5e. Figure 3.5c and 3.5f show the flow field during surging localized in the impeller and diffuser, respectively. Furthermore, the flow field disturbances make it difficult to obtain the phase slip behavior. Two-phase phenomena at surging inception and surging onset will be further discussed in Chapter 6.

High-speed videos are imported to the bubble analysis software in order to track the bubble displacement, acceleration, and velocity. The tracker is set to focus on the center of mass of a single bubble. As identified earlier, the tool shows to be limited in terms of the comprehensive flow disturbances, varying refraction factors, bubble shadows, and strong phase interaction. The bubble behavior is characterized by wobbling motion (see Figure 3.2) and clusters (coalescing bubbles), complicating the bubble trajectory [11]. With regards to the interactions, the tracker loses its target and the process

dismisses.

In agreement with Professor Hugo Atle Jakobsen professor at Department of Chemical Engineering at NTNU, a sufficient alternative would be to use the image processing analysis in Matlab. Perez reports that the software is advantageous in terms of image-processing abilities, flexibility in combining algorithms, and the potential of creating complex data structures [6]. This task, will however require more programming skills and available time, and should be considered in further work.

The experimental work reveals that phase slip behavior is dependent on multiple parameters. The most important are the GVF, rotational speed, and flow rate. The current flow visualization technique is satisfactory in order to identify the flow pattern and capture specific flow phenomena such as zones of gas accumulation and recirculation. On the other hand, the available visualization becomes limited when it comes to evaluating the physical flow mechanisms and transients at partload. Further documentation of phase slip would require more advanced visualization techniques, able to measure essential properties such as phase velocity, void fraction, and phase density which would give a more complete understanding of the flow mechanisms.

3.4 Summary

Visual investigations have resulted in a successful bubble tracking at the multibooster inlet section. Bubble tracking is also a promising in order to improve computational algorithms and two-phase models. The tracking captures the bubble motion as well as the bubble shape variations. However, exact correlations of the influencing effects still remain to be obtained. Body forces (centrifugal and Coriolis), drag force, and transversal acceleration fields are considered as the main influencing mechanisms. In order to confirm the assumptions, more advanced visualization and measurement techniques, such as LDV (Laser Doppler Velocimetry) and PIV (Particle Image Velocimetry) should be installed.

The bubble tracking software, which was originally intended to analyze the bubble behavior, shows to be sensitive due to the complex flow field. The tracker loses the bubble target immediately when the bubble contour changes. Other methods should be considered in future work, such as image analysis in Matlab.

Available studies regarding phase slip indicate that the research field is in an early stage for multiphase pumps. An extensive test campaign should be conducted in order to improve the fundamental understanding of the phenomenon. Furthermore, this would be of interest to optimize the pump design to reduce the risks of phase separation.

At 1% GVF, the bubbles appear entrained in the continuous phase indicating

low phase slip. With the increase of GVF, the size and number of bubbles have shown to increase. Consequently, bubbles coalesce into larger bubbles obstructing the incoming flow. This will induce relative phase motion which further affects the pressure production across the pump negatively. Further discussion of the characteristic flow phenomena and mechanisms will be given in Chapter 6.

Chapter 4

Surging in Multiphase Pumps

As for a compressor, surging is an unwanted phenomenon also in multiphase boosters. The critical condition is associated with pump performance degradation and system instabilities. Consequently, this may lead to fatal economical consequences.

In order to ensure steady machine operation, the issues due to instability and surging mechanisms should be thoroughly studied to lay a foundation for design improvements. Several studies are reported in literature, predicting surging through published correlations, but the lack of theoretical basis is a limiting factor.

This chapter will present some of the previous investigations in terms of an extensive literature review, aiming at documenting approaches to define and describe surging. It should be noted that the pump design and facility setup reported in literature will vary from the multibooster design, and care should be taken, especially, when considering numerical results stated in this chapter.

4.1 Previous Investigations

Prior experiments conducted through the PhD project "MultiBooster Performance" at NTNU, have been reported in [3, 1, 2], and will be the main contribution to this thesis.

Serena reports that flow recirculation zones blocking the channels play a major role in the unsteady machine operation [3]. By studying the multiphase mixture behavior, the phase distribution is governed by the balance between

the body forces and local pressure gradients [3]. Developing gas pockets close to the blade pressure surface (PS) are observed, due to coalescing bubbles and flow deceleration. In other cases, observations by flow visualization show that buoyancy effects lead the gas towards the suction surface (SS). The bubbles tend to coalesce and form gas pockets, blocking parts of the channels for the entering flow. Eventually, the pump recovers and the gas obstructions are swept away. This regime indicates high pulsations due to pressure and flow rate.

Lea and Bearden [26] investigated the detrimental effect of free gas in a submersible centrifugal pump. This was principally an experimental work and no correlations or models to account for the observations were presented. The experimental research considered tests with increasing gas fractions. A severe performance reduction and system instabilities were obtained for a gas fraction exceeding approximately 11%. This condition was termed surging. Further investigations showed that increasing the gas would result in pump gas-locking. The authors observed gas-locking to occur at lower GVFs operating with higher viscosity fluids, diesel-CO₂, compared to air-water. Furthermore, results showed an increased pump capability with higher intake pressures. In addition, the tests were performed considering a radial impeller and mixed-flow impeller, where the latter showed to have the best capability.

Experiments conducted on the multiphase booster indicate a reduced pressure production and increased system instability with the increase of GVF.

Patel and Runstadler [4] performed a qualitative experimental investigation of two-phase behavior. They observed that by increasing the GVF will increase the phase slip, which causes bubbles to coalesce forming large accumulations of gas within the impeller. The flow regime resulted in a high head degradation and tendencies of phase separation. Ramberg reported in [40] that the onset of surging depended mainly on the gas-liquid density ratio and gas volume fraction. The author relates the operating condition with a negative pressure gradient, as well as heavy pressure pulsations. Surging tests led the pump into "surge cycles" causing sudden discharge pressure oscillations. Tendencies of phase separation in the channels and gas accumulations close to the pump inlet, were detected. The phase separation induced channel obstructions leading to flow deceleration (liquid in particular), indicating a highly unwanted operating condition.

Two-phase models have been developed in order to predict flow instabilities.

Bratu [5] proposed a 1-dimensional analytical model based on a modified Fronde number with respect to the body forces (Coriolis and centrifugal acceleration) due to the curvature radius. The model considers the variations in phase slip, void fraction, phase separation effects, and curvature acceleration. Sun [9] reported a simplified theoretical model to predict ESP pressure

and void fraction distributions within the hydraulic channels. This model are also used in predicting surging and gas-lock conditions.

Surging tests performed in this thesis show strong flow field fluctuations and bubble coalescence, leading to higher risks of flow separation.

Murakami et al. [33] observed the bubble behavior using a high-speed camera together with a stroboscope on a centrifugal pump operating with air-water. They reported no bubble accumulation zones for void fractions below 4%, but exceeding void fractions of 6% led to accumulation zones and cyclic system vibrations. This condition was termed surging by Lea and Bearden [26]. Uchiyama et al. [35] associated the pump head breakdown with a flow pattern transition from bubbly flow to a "slug-flow-like" flow pattern initiated by a critical void fraction. Furthermore, Duran et al. [24] observed severe flow fluctuations during surging in a electric submersible pump. The authors predicted surging by observing a specific flow transition; initiating from an unstable bubbly flow pattern to an established elongated bubble pattern.

Sachdeva [39] proposed a hypothesis indicating that the onset of surging occurred due to the occurrence of zero gas flow velocity in the impeller. The author reported, in agreement with Barrios et al. [31], that the pump breakdown to be a consequence of the inlet gas pocket phenomenon. Subsequently, Estevam [44] observed the pump breakdown in agreement with the hypothesis regarding the inlet gas pocket [39, 33]. Based on the theory by Murakami and Minemura [33], Estevam [44] observed that the bubble size was increasing with the increase of volumetric gas fraction. The bubbles held a critical size between 2 - 3 mm at surging.

Based on Estevam's [44] observations, Prado [34] proposed a correlation between surging and the bubble size. This correlation could be explained through the influencing forces on the bubbles. Consequently, this was performed on bubbles inside the impeller by using Newtons law and ODE instability theory. Prado studied the condition triggering the unstable condition due to the radial position of a bubble with subject to the centrifugal force. He reported that large bubbles reached an equilibrium position (like a satellite around earth) within the impeller flow.

Gamboa and Prado [19, 18] describe surging inception to be dependent on the void fraction, suction pressure, liquid flow rate and the specific pump geometry. They concluded that the surging always coincides with a pump head breakdown indicating a severe change in the pump performance. Accordingly, they reported the rotational speed and the intake pressure to be critical factors due to the surging inception.

Gaard [41] performed studies on bubble behavior in bubbly flows. Phase slip, gas pocket zones and phase separation intensify with increasing GVF. In addition, the author reported the bubble size to increase according to the increasing GVFs. Consequently, this led to a higher flow obstruction and

pump performance degradation.

Barrios and Prado conducted an extensive study in order to document the dynamic flow behaviour in a mixed-flow ESP [29, 30, 31]. The authors reported, also, that the bubble size and bubble coalescence were increasing with the gas void fraction. Furthermore, based on the criterion of bubbles with a specific size (as identified by Estevam in [44]) becoming stagnant at a radius equal to the pump intake, they developed a 1-dimensional mechanistic model to predict the surging onset. Their studies comprise a pump design quite equal to this thesis test facility, but with a less complex transparent casing. In addition, Barrios et al. [14] developed a 3-dimensional CFD model considering bubble size and bubble drag coefficient, in order to analyze the onset of surging. The results from the simulations were in agreement with the experimental data in [29]. They concluded that a successful utilization of CFD codes requires a fully understanding of the flow physics inside the impeller channel.

4.2 Summary

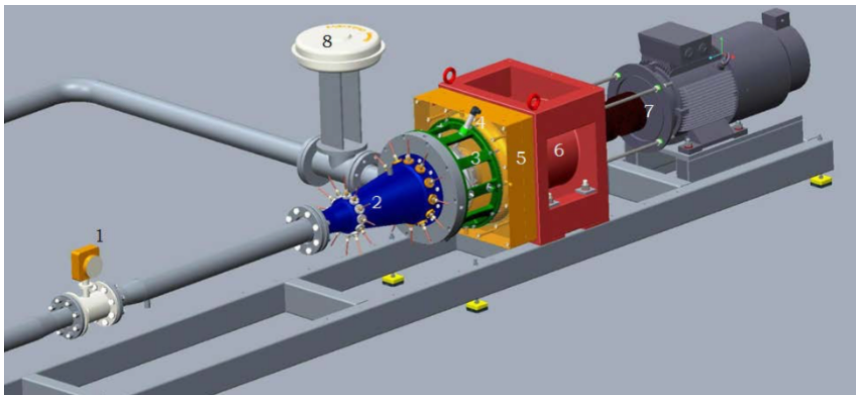
The literature review reveals various approaches of studying surging in multiphase pumps; experimental, theoretical, and computational. It is difficult to state if some method is better compared to the other, but the approach with respect to, respectively, experimental "step-by-step" investigations, accompanied with computational simulations are expected to deliver promising results. An example of this method can be found in [14, 31, 18], showing one of the most recent studies on this field of topic.

Surging and two-phase instabilities in multiphase pumps are characterized by complex mechanisms. Bubble behavior [29, 34, 41], flow pattern impact [26, 4], and recirculation zones [3] are some of the phenomena studied with regards to the topic. The majority of the studies found, base their investigations on empirical correlations, such as coalescing bubbles, sudden pressure drop, channel obstructions, and intensifying fluctuations. Currently, there have not been obtained an exact solution to describe and understand the two-phase mechanisms causing surging. Further evaluation of the unstable condition due to this thesis work, will be given in Chapter 6.

Chapter 5

Test Facility and Experimental Method

The novel test facility at the Thermal Energy Department at NTNU, reproduces the full-scale MultiBooster at Aker Solutions – Tranby (Oslo). A test campaign has been conducted in order to valuable information regarding the multibooster instability operating conditions. Consequently, the tests are expected to give an improve understanding of the flow fundamentals in order to avoid the unwanted flow regimes. The experimental work is performed in cooperation with the PhD project, "MultiBooster Performance".



- | | |
|-----------------------------|------------------------|
| 1 - Water Flow Meter | 5 - Volute |
| 2 - Air Injection Section | 6 - Bearing Pedestal |
| 3 - Pump Transparent Casing | 7 - Coupling and Motor |
| 4 - Local Instrumentation | 8 - Choke Valve |

Figure 5.1: Test Rig at Thermal Energy Department, NTNU

A list of the main components constituting the test rig is given in Figure 5.1.

More information about the design, components limitations, and instrumentation is found in [2] and Appendix.

5.1 Test Facility

The test facility is designed in order to permit a detailed flow field analysis of the hydraulic channels, required for further design optimization. It is compatible with machine adjustments such as varying the impeller tip clearance, impeller replacement, and various visualization and measurement techniques. This is of great value in order to assess and document the machine operation. Figure 5.2 represents a simplified P&ID of the test facility.

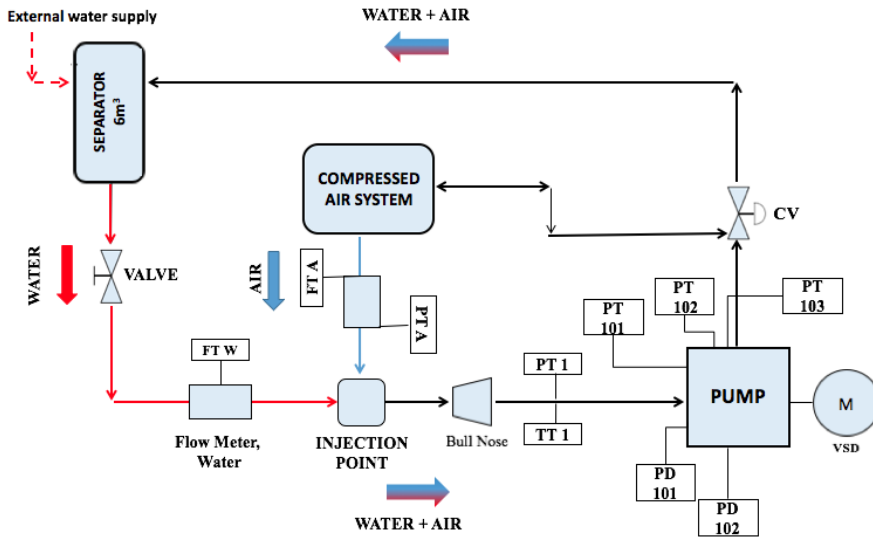


Figure 5.2: Simplified P&ID

A 6 m^3 water vessel is connected to an external water supply and works as a horizontal buoyancy separator at atmospheric pressure. The separator is sized in order to provide a certain retention time fulfilling the requirements of delivering a fluid with non-visible gas. The working fluids are chosen to be water and air due to low risk perspectives. The phases are separately led into the injection point upstream of the pump. Liquid and gas flow meters are installed, respectively, to acquire the upstream flow rates of both phases.

The single stage pump has an un-shrouded semi-axial impeller controlled by a variable speed drive (VSD). Pressure sensors (described in Section 5.3.1) are installed in order to analyze the flow field pressure evolution. In addition, temperature sensors are included to give temperature measurements in order

to conduct experiments at the same flow temperature. In addition, the temperature sensors help ensuring a safe operation by notifying overheating of the bearings and of the PMMA casing. Air injection is performed through a compressed air valve system, located at the injection point in front of the bull nose (see P&ID, Figure 5.2). Furthermore, the control valve (CV) is connected to the compressed air system regulating the total flow rate.

5.1.1 Risk Assessment and Operational Limitations

In order to be perform experiments, a necessary risk assessment has been conducted by Alberto Serena together with the Thermal Turbomachinery Lab personnel at NTNU. The assessment fulfil the HSE requirements for indoor building testing with respect to reduce human risks and damage of the lab equipment. The multiphase booster operating limitations are listed in Table 5.1.

Table 5.1: Multiphase booster limitations

Variable	Range
Speed	500 – 2500 rpm
GVF	0% – 90%
Δp_{max}	8 bar(a)

5.2 Visualization Equipment

The high-speed camera provides a satisfactory optical view of the hydraulic channels, allowing visualization of characteristic flow instabilities and surging mechanisms. However, the flow visualization has shown to be challenging when considering partload operation. The flow field is characterized by high gas contents and flow transients. In addition, a complex pump design, varying refraction factors, and light reflections of the metallic parts serve a challenge to the flow visualization.

The PMMA casing is 360° transparent, and with only one camera available, only a single part of the pump has been considered. It should be noted that asymmetric flow effects will occur, and a complete flow field analysis would thus require to cover a broader part of the pump.

More advanced visualization techniques such as Particle Image Velocimetry (PIV) and Laser Doppler Velocimetry (LDV) are expected to give a more complete flow analysis in order to document the unsteady machine behavior. Also, a 3-dimensional flow analysis would have been of great value, in order to document spatial flow field variations.

5.2.1 Direct Flow Visualization

Flow visualization is performed through a high-speed camera, Photron PCI 1024 with a 50 mm lens by Nikon, together with a 400 W light projector. Table 5.2 shows the main visualization instruments.

Table 5.2: Visualization equipment

Instrument	Model	Producer
Camera	Photron PCI 1024	Photron
Light	Dedolight 400D	Dedolight
Lens	50mm	Nikon

As mentioned above, the camera is set to focus on a single part of the pump, either the inlet, channel, or the diffuser. In order to study the multiphase booster flow phenomena, a succession of sharp images for every blade passage is needed.

The camera resolution and record time are adjusted according to the specific test performed; low GVF tests at steady flow require lower resolution and record time compared to tests at surging where comprehensive flow phenomena are considered. Furthermore, longer record time and high camera resolution introduce a challenge due to file size and data storage.

Various camera and light settings have been performed in order to achieve videos of a satisfactory quality. The shutter time and objective aperture determine the exposure time in which light reaches the digital camera sensor, playing a key role in order to acquire bright images with low reflections. Table 5.3 lists the high-speed camera and light settings used during the experimental work.

Table 5.3: Camera and light settings

Model	Photron PCI 1024
Maximum resolution	1024 × 1024 pixel at 1000 fps
Set resolution	384 × 352 pixel
Set frames per second	1500 – 6000 fps
Shutter time	140 μ s
Recording time	2 – 6s
Focal length	50 mm
Objective aperture	$f/4.0$
Camera height	110 cm
Light height	183 cm

5.3 Data Acquisition Equipment

A complete data acquisition system allows to control operative parameters and analyze vital flow field parameters. Data are monitored and logged through the laboratory computer. Table 5.4 lists the most important instruments used in the experiments.

Table 5.4: Main Instruments

Tag-ID	Instrument	Range	Model
PT	Pressure Transmitter	0 – 7 bar(a)	PCE-28 Smart
PD	Pressure Transmitter	0 – 2.5 bar(a)	PCE-28 Smart
TT	Temp. Transmitter	0 – 60 °C	CT 14
CV	Choke Valve	0 – 200 $\frac{m^3}{h}$	Logix 510 si
FT A	Flow Meter, gas	0 – 200 $\frac{m^3}{h}$	In-flow High-Tech F-106A1
FT W	Flow Meter, liquid	0 – 200 $\frac{Nm^3}{h}$	FEV112
VSD	Variable Speed Drive	55/75kW, 400V	iDrive

5.3.1 Pressure Sensors

Five pressure sensors, two dynamic (PD) and three static (PT), are indicated in Figure 5.3 with their respective tags and positions.

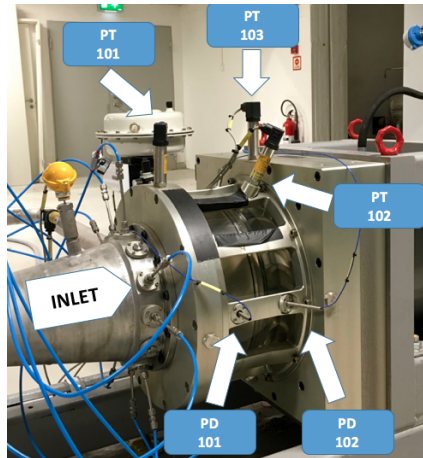


Figure 5.3: Placement of dynamic (PD) and static (PT) pressure sensors

The sensor placements are chosen specifically to analyze the flow pressure evolution along the hydraulic channels, localized at the impeller inlet and outlet, and at the diffuser outlet. The fast-response and the short term static pressure probes can easily be relocated to the position most suitable with regards to the test performed. Sensor locations are however kept constant during this thesis work.

The fast-response piezoelectric pressure sensors (PD) by PCB[®]. The sensors are located at the inlet and outlet of the impeller, permitting pressure signals acquired at 1,5 kHz through a dedicated amplifier. The static pressure signals (PT) are acquired through an analog current signal with a frequency of 10 Hz.

5.3.2 Data Logging System

Operative parameters and data acquisition are controlled through a data logging system in LabVIEW. The operator screen together with the most important features are outlined in Figure 5.4.

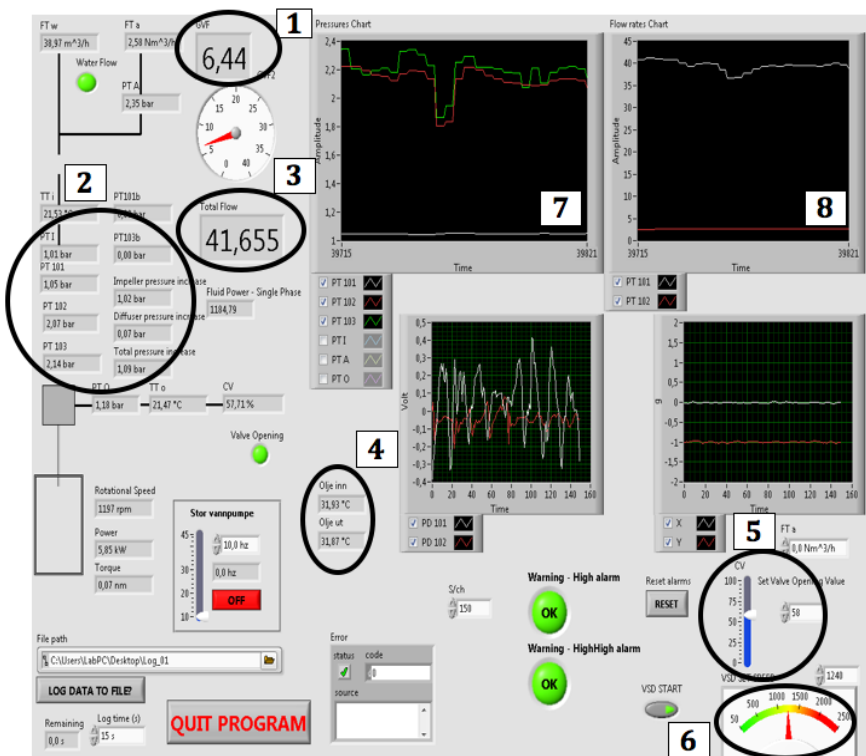


Figure 5.4: LabVIEW screen

The most important functions in LabVIEW are listed below:

1. GVF
2. Pressure measurements
3. Volumetric Flow Rate
4. Oil temperature (bearings)
5. Control Valve: 100 % (fully open) – 0 % (fully closed)
6. Rotational Speed
7. Monitored Static Pressure
8. Monitored Dynamic Pressure

5.3.3 Data Processing

With regards to the thesis main objective, a method for relating pressure pulsations to flow mechanisms is presented. The data processing software, NI DIAdem, is compatible with synchronizing videos with pressure signals. Thus, local and overall flow field behavior captured of flow visualization can be analyzed through pressure data. Care should be taken when implementing the videos to the analysis software. The recordings should correspond with the pressure signals. Also, the presence of two-phase flow introduces challenging aspects due to sources of errors, occurring to be a challenge when operating at high GVFs, due to random pressure pulsations, accompanied with a dampening effect with regards to the gas compressibility. Error analysis is not of main interest in this thesis, further information regarding the topic and relevant assumptions are reported in [7].

5.4 Experimental Procedure

All experiments are performed in agreement with ISO 9906 and the permissible uncertainties reported in [2]. The visualization and data-acquisition are described in Section 5.1 and 5.3.

Tests have been conducted in order to acquire a broad collection of data to study the multibooster surging and related mechanisms. The experimental test matrix bases on the following variables:

- Fraction of nominal flow rate: $q^* = \frac{q_t}{q_{nom}}$ [%]
- Gas Volume Fraction: GVF [%]
- Rotational speed: n [rpm]

The experimental procedure is inspired by previous experimental surging approaches [2, 3]. The test procedure is described in terms of the following steps:

1. The multiphase booster is adjusted to obtain the desired flow rate through the control valve (CV), when operating at single phase.
2. Gas is injected to the flow, where the value should be within 1% with respect to the target value.
3. The flow rate is adjusted through the CV with respect to the injected gas. The value should be within 1% with respect to the target value.
4. Video recording and data logging
5. 2. and 3. are repeated until certain flow instabilities are observed through the pressure signal monitoring and flow visualization.
6. The specific test continues until the pump becomes gas-locked.

Seen of the test matrix, test 1 – 3, consider flow visualization at the impeller inlet, rotating channel, and diffuser channel, respectively.

The test points performed are stated in Table 5.5.

Table 5.5: Experimental test matrix

Test number	Test name	Test points
1	Surging test: Inlet	n : 900 – 1200 – 1800 [rpm] q^* : 70 – 60 – 50 [%] GVF: 2% – surging
2	Surging test, Channel	n : 900 – 1200 – 1500 – 1800 [rpm] q^* : 80 – 70 – 60 – 50 [%] GVF: 2% – surging
3	Surging test, Diffuser	n 900 – 1200 – 1800 [rpm] q^* : 70 – 60 – 50 [%] GVF: 2% – surging

It should be noted that the incremental steps of GVF are adjusted with respect to the operating condition; in steps of 2% for steady machine operation, 1% for relatively small pressure variations, and 0.5% for highly unsteady operating conditions, where distinct pressure variations are observed. Experimental results indicate that surging occurs for GVFs between 7% and 20% dependent on the rotational speed and flow rate.

5.5 Rig Evaluation and Error Sources

The nature of multiphase flow mechanisms introduce challenges due to measurement accuracy and visualization. It should be noted that this thesis

experimental results will depend on the impeller and diffuser design, as well as the specific facility setup.

The location of pressure sensors gives an overall description of the flow field pressure evolution. However, a dynamic pressure sensor placed at the diffuser outlet would improve the accuracy of the pressure analysis. Pressure sensors placed at each quadrant of the pump would reduce the errors due to asymmetric flow field.

The test set-up gives a satisfactory overall access with regards to data acquisition. The 360° transparent casing provides a unique opportunity to analyze the flow field within the hydraulic channels. Furthermore, the setup is limited when it comes to measuring the phase velocity as well as the fluid properties (density and viscosity). Such measurements would be desirable in terms of bubble behavior and phase slip analyses. More advanced measurement and visualization techniques, such as Laser Doppler Velocimetry or Particle Image Velocimetry, should be considered in further researches.

As surging is approached, the experimental work indicates high irregularities due to pressure and flow rate variations. This results in higher channel obstructions, affecting the machine operation. Consequently, the pump capability of handling gas, has shown to vary slightly from test to test. An exact reason is currently not obtained, but it would be desirable to analyze the impact of changing flow temperatures. Features due to pre-whirl and gas injection mixing length should also be considered to improve the phase mixing. This is expected to provide a more homogeneous inlet flow, assumed to give test results of higher consistency.

An automatically adjusted gas injection system would improve the accuracy of gas injection. The current injection system, with manually employed valves, is difficult to maneuver where fine adjustments are required.

Chapter 6

Results and Discussions

The applicable operating range of multiphase pumps is limited. In accordance with previous researches, the machine operation is unstable at low flow rates and increasing gas contents. Consequently, the first part of this chapter explores the surging inception and evolution through an extensive test campaign, intended to document some of the related two-phase instabilities. The analyses are conducted through a data acquisition system and flow visualization. Subsequently, the high-speed videos and pressure data are analyzed in the data processing tool described in Section 5.3.3.

Surging is associated with intensifying system instabilities, affecting the pump performance and system stability. Machine breakdown and downtime, especially in subsea installations, result in high economical losses. A detailed understanding of the mechanisms is thus essential in order to avoid the unstable condition. The operating condition will damage the machine and cause propagating vibrations through the compression system. In order to assure safe and reliable operation one should be able to detect surging. The second part of this chapter presents a method to detect surging inception based on the correlation between GVF and discharge pressure variations.

6.1 Multiphase Booster Instability

Surging analysis is apparently a complex field of research. Adding an extra phase to the flow, complicates the physical mechanisms dramatically. The operating condition is explored through experimental tests comprising various combinations due to increasing GVF, where the flow rate and rotational speed are maintained constant. Higher rotational speed improves the pump capability but makes flow visualization more challenging in terms of intensified phase interaction. When operating at high gas volume fractions, the flow is characterized by high flow irregularities. Momentum transmission

due to phase interaction causes transients characterized by phase separation, bubble coalescence, rotational and transversal effects, and secondary flows.

Flow visualization accompanied with data processing have resulted in detection and analysis of specific flow phenomena. The main observations are listed below:

- Inlet gas pocket
- Channel gas pocket
- Empty-of-gas channel
- Diffuser recirculation zone

The experimental procedure is described in Section 5.4.

6.1.1 Surging Inception

The surging inception is studied through experiments considering stepwise increment of the GVF, with maintaining the rotational speed and flow rate constant. The tests are conducted for three different rotational speeds (900 – 1200 – 1800 rpm) at partload in agreement with the test matrix listed in Table 5.5.

With the increase of GVF, the flow field oscillations increase accordingly. Furthermore, the number and size of bubbles are observed to increase and cause channel obstructions. Flow obstructions are recognized by bubble coalescence, gas pockets, and recirculation zones. Moreover, when the GVF is too high, the pump appears to be fully blocked by gas (gas-locked).

The data processing tool synchronizes pressure signals with high-speed videos, expected to analyze potential correlations between the visual instabilities and pressure variations. The curves seen of the bottom graph display the dynamic pressure signals, and the upper right graph shows the static pressure values ones. The purple and blue colored curves represent the impeller inlet and outlet pressure, respectively. Figure 6.1 – 6.3 show the flow visualization when surging is approached under the following conditions: 1800 rpm, 50% q^* , and 1%, 5% and 10% GVF.

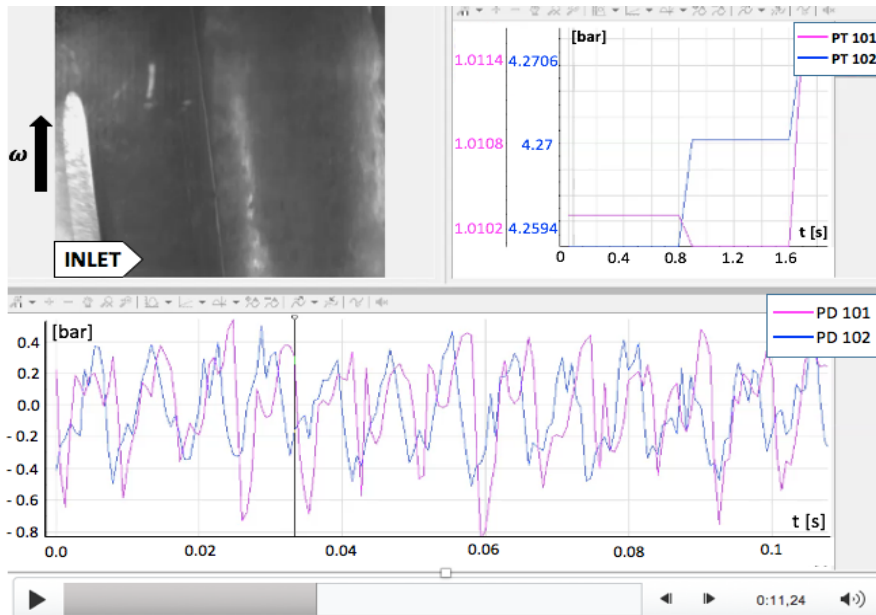


Figure 6.1: Approaching surging, 1% GVF

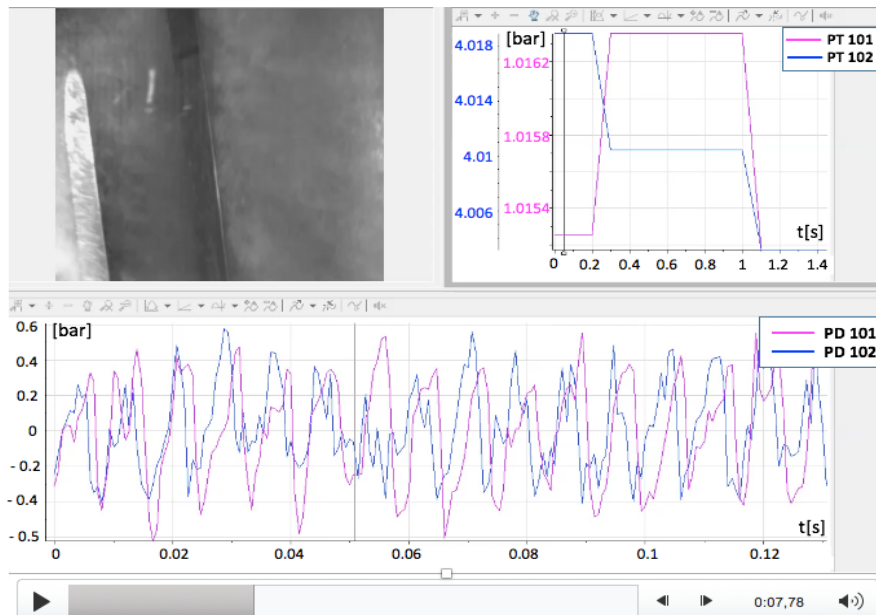


Figure 6.2: Approaching surging, 5% GVF

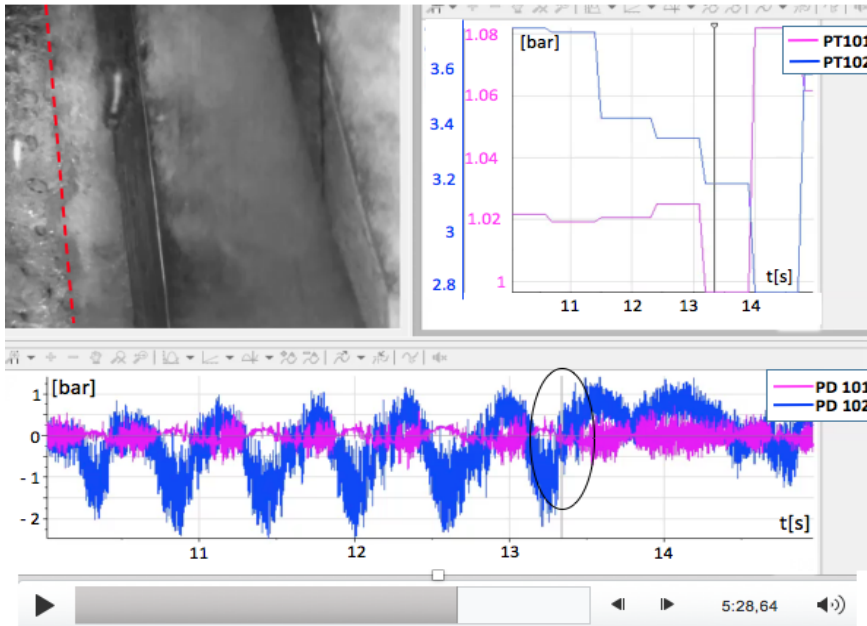


Figure 6.3: Surging onset, 10% GFV

As identified of the pressure signals, the flow field instabilities show to increase with increasing GVF. The operation condition appears stable at 1% GVF, due to well mixed phases with no sign of phase slip. At 5% GVF (see Figure 6.2), the pump still manages to deliver a steady flow, indicated of the low pressure deviations. However, intensified fluctuations have been observed, both of flow visualization and eye view perspective.

Figure 6.3 shows a oscillating pressure evolution at the impeller outlet, indicating a highly irregular operating condition. At this condition, the flow behavior appears irregular and difficult to predict and analyze. The pump capability of providing a continuous flow shows here to reduce. Gas and liquid, respectively, are observed to be in separate phases moving relative to each other. This indicates that phase slip occurs as a consequence of the channel obstructions. Furthermore, the channel obstructions cause flow deceleration, leading to a stratified flow pattern and stabilized bubbles (seen to the left of the red dashed line in Figure 6.3). The isolated bubbles are visualized at relatively high GVF, flowing towards the blade suction side. Furthermore, based on visual observations this flow pattern is recognized as highly unstable with regards to the bubbles forming a gas pocket. This trend will be further discussed in Section 6.1.2.

The dynamic pressure curves in Figure 6.3 indicate the pressure evolution during surging at 1800 rpm. The curves show a regularity due to the cyclic pressure oscillations. Accordingly, the high-speed video shows alternating

flow field corresponding with the pressure signal evolution; approaching a local minimum, the flow picture appears whiter due to high gas influence. This is in agreement with the pump performance theory, indicating that pressure reduction when processing higher gas fractions. In addition, annular flow is observed in terms of the liquid film adhered the plexi, where the main flow is composed of gas and liquid drops. In the other case, towards a local maximum, the flow field appears darker, indicating lower GVF, providing a more suitable operating condition.

The multiphase flow characteristics and the system stability have shown to be dependent on various parameters; gas volume fraction, rotational speed and flow rate. Experimental tests show an overall intensification of the system instabilities and flow irregularities. The increase of GVF leads to changes in the bubble behavior as well as the differential pressure across the pump. Trends of bubble coalescence and channel obstructions seem to play major role in the unsteady flow behavior reported here. However, the pump shows to be capable to operate even though the condition appears as highly unstable (seen by Figure 6.3. Tests at 900 rpm and 1200 rpm are in accordance with the trends. The condition will be further discussed in the next sections.

6.1.2 Bubble Coalescence and Gas Pockets

In order to document the surging inception and evolution, numerous tests at different GVFs and flow rates have been conducted. Bubbles are seen to grow in size and number with increasing GVF. Because of the low density, the majority tend to flow towards low pressure zones and accumulate into pockets of gas. These accumulations form masses of stabilized bubbles, obstructing the incoming flow. Gas pockets have been observed both at the impeller inlet and inside the impeller channels.

Figure 6.4 captures a static gas pocket localized at the pump inlet section. The phenomenon has shown to intensify during surging for all test speeds.

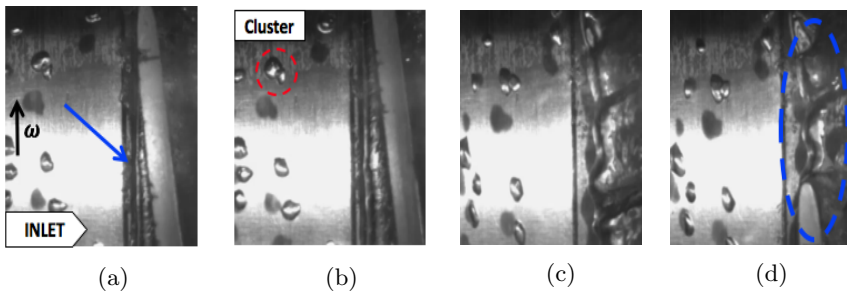


Figure 6.4: Static inlet gas pocket at 900 rpm and 70% q^*

The developing gas pocket in Figure 6.4a originates at the lowest pressure zone, the blade suction side (SS). The gas pocket occupies the channel inlet and becomes static until the pump manages to recover. As a consequence of the gas pocket blockage, liquid flow tends to decelerate and accumulate in front of the obstructions. Furthermore, if the obstruction is too strong, the pump will become gas-locked.

In Figure 6.4a, the large entering bubbles have either a relatively spherical or elongated shape due to drag induced by the impeller. The tests prove an intensifying bubble coalescence, when approaching the surging onset. Figure 6.4b depicts an example of two coalescing bubbles (termed bubble cluster in [11]), indicated with a red circle. As the bubbles approach the impeller, the incoming flow experiences a counteracting force (indicated by the vertical elongated shape in Figure 6.4c and 6.4d). As identified in Section 3.1.3, the shape changes with respect to the influencing forces; the velocity difference between the phases leads to irregular phase acceleration and gas accumulation [17].

Estevam [44] and Minemura et al. [33] observed a stage head breakdown in a mixed-flow pump as a consequence of an inlet gas pocket. Additionally, Barrios and Prado [31] defined surging as a sudden pressure drop depending on the rotational speed as well as the liquid and gas flow rate. Also, Barrios studied the surging transition, and concluded that bubbles exceeding a certain diameter would become stagnant in the impeller inlet region. Furthermore, she reported that bubbles were coalescing into gas pockets which caused a sudden pressure drop across the pump. Focus should be given in order to study the correlations between the bubble size and the occurrence of gas pockets.

Channel Gas Pocket

Gas pockets have also been observed inside the impeller channels. Similar to the inlet region, the number and size of bubbles are observed to increase with the increasing GVF. Furthermore, higher GVFs result in increased collisions between the bubbles. The collisions make bubbles coalesce into larger stabilized bubbles (spherical) in the channel for a certain period of time. Consequently, these bubbles have in some cases shown to form a gas pocket, either at the suction side (SS) or pressure side (PS) of the impeller blade. Figure 6.5a and 6.5b show, respectively, isolated bubbles and gas pocket at the blade suction side under the following surging condition: 1200 rpm, 70% q^* and 10% GVF.

Figure 6.5 shows a succession of images where the bubbles flow, closely gathered, towards the blade suction side and form a gas pocket. The gas pocket pictured in Figure 6.5b affects the flow negatively in terms of the channel obstruction and by changing the shape of the impeller channel. A change of the available flow area might cause losses in terms of discrepancies from the original hydraulic channel design.

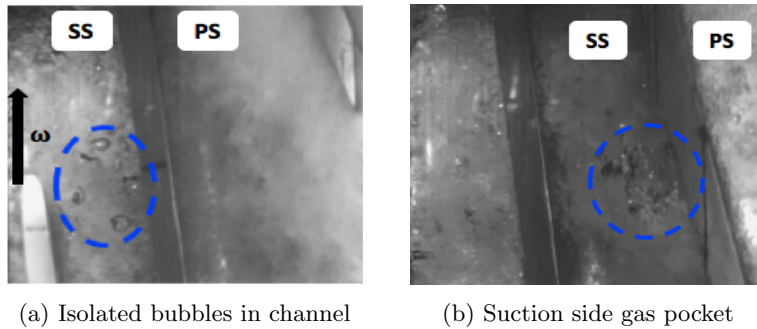


Figure 6.5: Surging at 1200 rpm and 70% q^*

Further studies are conducted through data processing in order to obtain correlations between the gas pocket and the delivered pressure. Figure 6.6 depicts a gas pocket (inside the blue circle) located at the impeller outlet PS (0.8 chord) synchronized with pressure signals at the impeller inlet (purple curve) and outlet (blue curve).

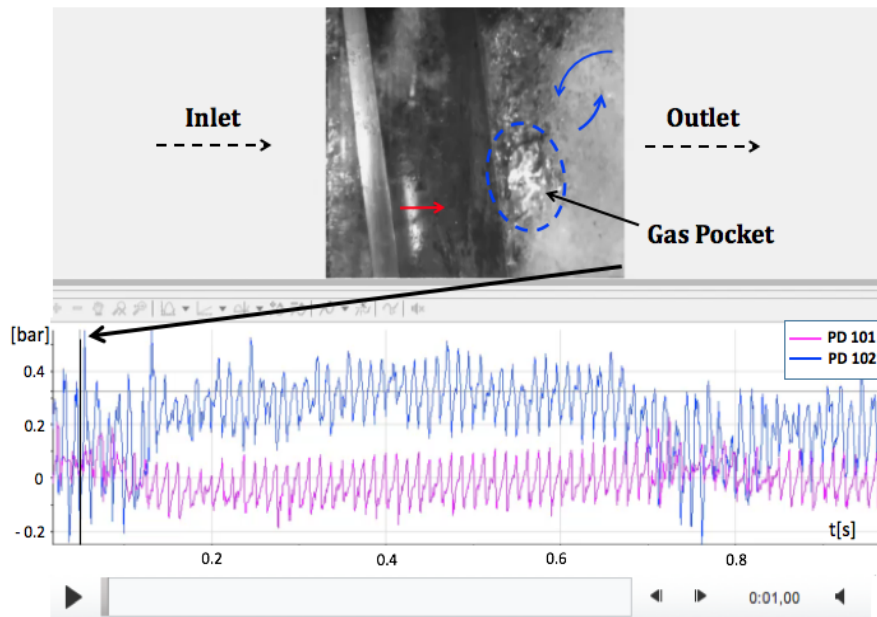


Figure 6.6: Data processing – Surging at 1200 rpm and 70% q^*

The blue ring located at the impeller outlet, marks the gas pocket adhered to the blade pressure side. Following, inside the impeller channel, the liquid (red arrow) and gas are observed as fully separated. When analyzing the pressure behavior, any exact judgments are difficult to give here. However,

in particular cases, a higher pressure peak corresponds with the following empty-of-gas channel (indicated of the black arrow in Figure 6.6). This could be explained by the liquid flow improving the operating condition.

Gas pockets are observed to occur both periodically and randomly with respect to time and position. At the surging onset, flow visualization shows repetitive static gas pockets close to the PS. Consequently, the gas pocket becomes unstable due to the approaching liquid flow and pushed through the channel. The sudden displacement leaves behind a white wake characterized by significant vortices. The procedure is illustrated in Figure 6.7.

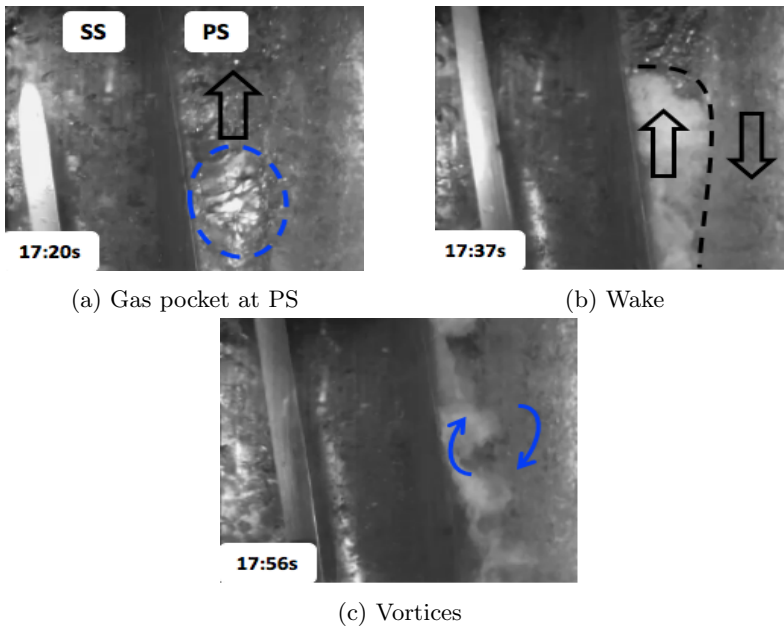


Figure 6.7: Surging at 1200 rpm and 70% q^*

An extensive white wake appears behind the gas pocket. The black line pictured in Figure 6.7b indicates a segregated flow pattern at the impeller outlet. The wake, enclosed by the interface line, is affected by the counteracting pressure gradient of the impeller and the flow to the right of the interaction line. The wake is influenced by counteracting forces, forming a characteristic vortex pattern that reminds of the "Kelvin-Helmholtz" instability phenomenon. This is originally caused by either shear forces acting in a continuous fluid or by velocity difference across the interface area between two fluids. The triggering mechanisms of the significant vortex pattern has shown to be difficult to give by the current experimental results.

The channel gas pocket phenomenon is observed during partload operation for flow rates between 70% – 50% q^* for all tested speeds, with variations due to position and time. Periodically occurring gas pockets have shown to

correspond with the empty-of-gas channel phenomenon in particular cases. Moreover, this is recognized by bubbles moving towards the lower pressure zones at the blade suction side, where they coalesce and appear stagnant for a short period of time. Furthermore, with the following revolution the bubbles are seen as gas pockets at the blade PS.

The test campaign accompanied with flow visualization and data processing have located a correlation where coalescing bubbles form into gas pockets. In particular cases, both at surging inception and evolution, the one flow phenomenon lead to the other phenomenon; (1) coalescing bubbles forming gas pockets, (2) gas obstructions increase the risk of phase separation. Data processing indicates that the presence of gas obstructions causes flow instabilities due to high pressure variations, affecting the pressure production reliability across the pump.

The gas pockets have been observed in different shape, size, and location, dependent on the operating condition. Higher GVFs and lower flow rates are associated with larger gas accumulations. However, in order to determine the shape and location of the gas pocket, it would be desirable to perform an analysis of the influencing forces on the bubbles. The main influencing forces on an isolated bubble are illustrated in Figure 3.1.

6.1.3 Empty-of-Gas Channel

The empty-of-gas channel phenomenon has been explored for all test speeds at flow rates between 70% – 50% q^* . The phenomenon is intended to cause flow irregularities and strong pressure fluctuations, amplifying with the increase of rotational speed. Figures 6.8a to 6.8i show the phenomenon from start to end under the following condition: 900 rpm and 70% q^* at surging.

The red and blue arrows show the liquid and gas flow, respectively. In addition, the stagnant zones are marked with blue two-arrowed lines. It should be noted that the magnitude and direction of the arrows is scaled due to empirical observations by flow visualization.

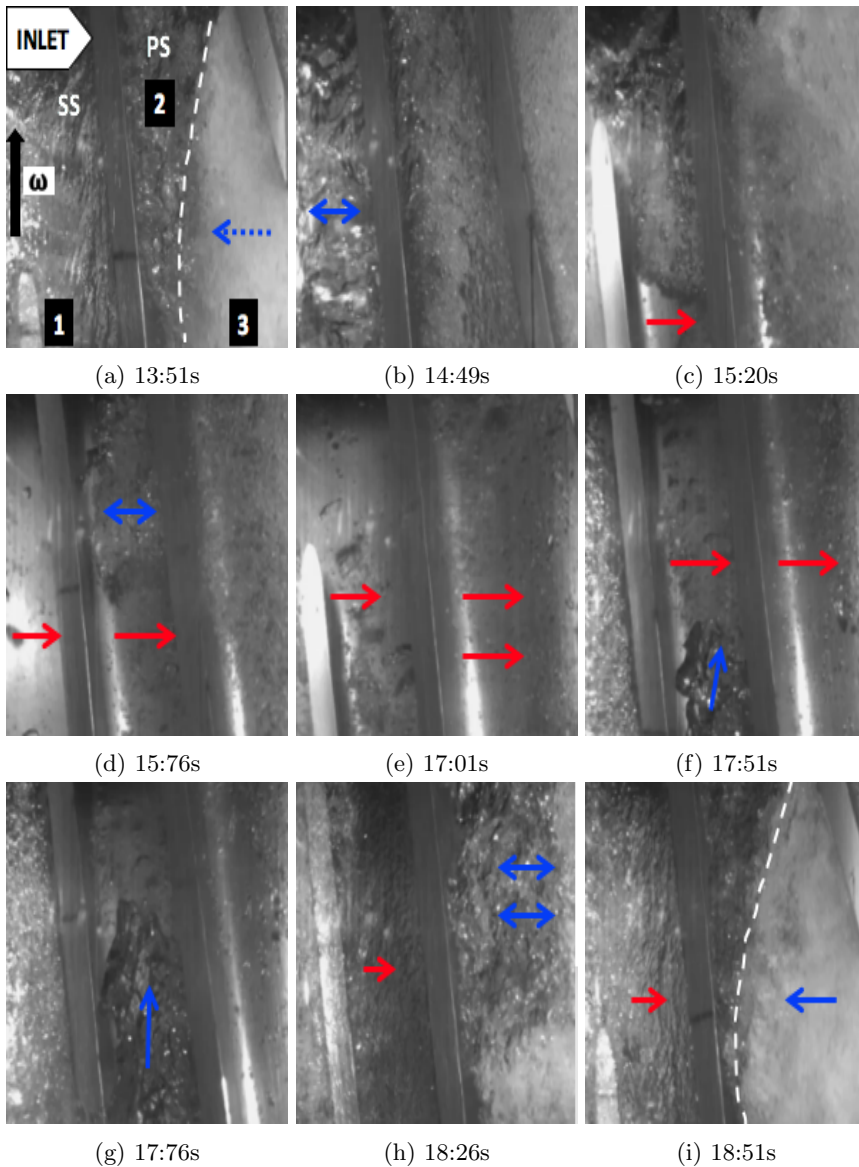


Figure 6.8: Empty-of-gas channel at 900 rpm and 70% q^* at surging onset

The succession of images gives an overall view of the irregular channel flow field during surging characterized of flow pattern transitions and phase separation. Figure 6.8a shows a segregated flow identified by three regions (inlet towards outlet of the impeller); (1) annular flow, mainly composed of gas in the main flow and liquid film adhered to the plexi, (2) gas pocket region localized at the blade pressure side at approximately 0.5 chord, (3) and the white region dominated by air. Moreover, the white zones at the im-

PELLER outlet indicates high flow disturbances due to the diffuser recirculation zones.

Figure 6.8b pictures the gas pocket zone at the impeller inlet (equivalent to the one in Figure 6.4d). Figure 6.8c – 6.8e, show the empty-of-gas channel phenomenon, identified of liquid filled channels. Data processing shows a correlation between the phenomenon and an improved operating condition (seen of the marked pressure peak in Figure 6.9). In particular cases, it appears two empty-of-gas channels in a row, which is seen of Figure 6.8d – 6.8f. From 0.4 to 0.6 blade chord, a sudden gas pocket flow entering from below and obstructs the channel passage, indicated in Figure 6.8f and 6.8g. Also, the gas density is much lower compared to the liquid density and is therefore more strongly influenced by the buoyancy force leading the gas towards the upper pump partition. In particular cases, this alternating sequence shows to be repetitive. In this case, the phenomenon occurs every 5th revolution over a certain period of time, causing flow instabilities propagating through the pump. Figure 6.8h represents the start condition, as in Figure 6.8a, showing the initiation of a new sequence.

The alternating liquid and gas channels are recognized from an eye perspective view as an annular gas ring moving forth and back [3]. Flow visualization has later identified the phenomenon as the sequence of alternating channels filled with gas and liquid, consequently. Obstructing gas decelerates the incoming flow, until the pump recovers and manages to remove parts of the blocking gas. The sequence becomes intensified during surging. In addition, the operating condition is associated with the last possible operating point for the multiphase booster; implying that further increasing the GVF will result in a gas-lock of the pump.

Furthermore, the flow rate and pressure across the pump fall down to zero. Also identified of the flow transition from unstable empty-of-gas channels towards annular flow during gas-locking. The multiphase flow during annular flow is characterized by high phase slip (seen of flow pattern map in Figure 2.3), representing a highly unwanted flow regime to the machine operation. The exact mechanisms behind the fluid dynamical transition is not currently obtained. A complete identification of the flow mechanisms would require a qualitative 3-dimensional flow visualization and phase velocity measurements.

Data processing synchronizes flow visualization with pressure signals, showing the dynamic pressure of the bottom curves, and the static pressure of upper right corner curves in Figure 6.9. It should be noted that the respective inlet and outlet signals have the opposite colors with respect to dynamic and static signals. Figure 6.9 shows the empty-of-gas channel synchronized with pressure behavior at 900 rpm and 70% q^* , recorded with a camera fps of 1500 Hz.

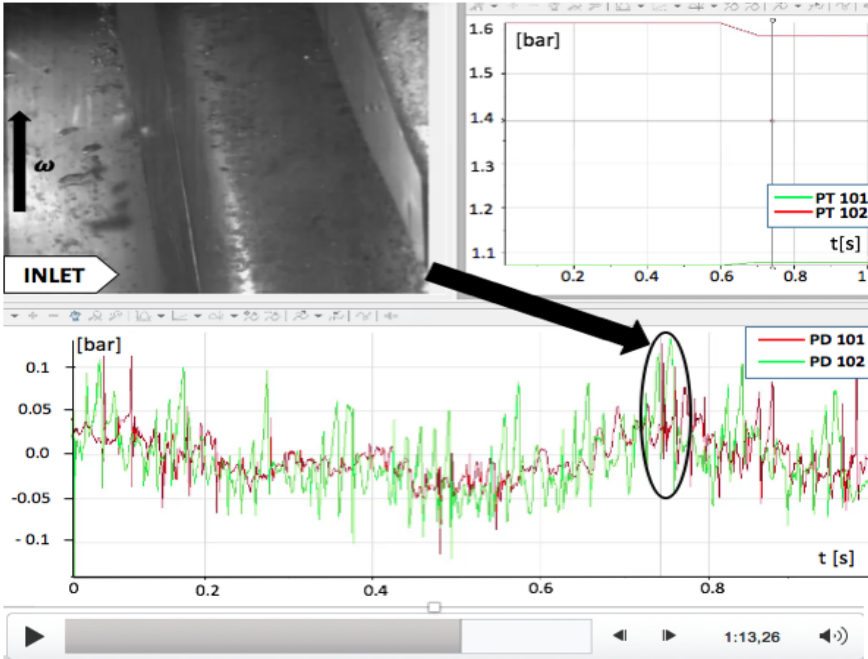


Figure 6.9: Data processing – 900 rpm and 70% q^* at surging

Figure 6.9 shows two empty-of-gas channels in a row. The black arrow indicates a sudden pressure peak, occurring correspondingly with the approaching liquid channels. The pressure amplitudes show to be highly dependent on the rotational pump speed; tests at 1800 rpm and 900 rpm under the same flow rate relative to the nominal one, reveal maximum amplitudes of 2 bar and 0.15 bar, respectively. This results in a ratio of 13.33 times larger maximum pressure amplitudes when comparing the two speeds. Accordingly, this relation marks that surging operation becomes more critical to the process system at higher rotational speed.

The alternating liquid and gas channels have shown to occur for all tests explored and cause strong flow field irregularities. As with the gas pocket phenomenon, the empty-of-gas pocket changes due to the operating condition. When approaching surging at lower flow rates, the visualization and data processing features the phenomenon to intensify. It would be desirable to detect the inception and axial-radial evolution of the alternating channel blockage, which are performed for surge in compressors, by the use of time-frequency signal analyses [43].

6.1.4 Diffuser Flow Investigations

The diffuser is the component where the flow is decelerated and kinetic energy is converted into static energy. An efficient diffuser design is here essential due to optimized pump operation. This section will study the main flow field characteristics inside the diffuser when approaching surging.

Flow separation is more likely to occur in bended channels [25]. Investigations reveal that bubbles coalesce into larger bubbles which may lead to gas pockets. Barrios reported that bubbles smaller than a certain diameter, to avoid coalescence and continue into the diffuser [31]. In these experiments, isolated bubbles are visualized for very low gas fractions. However, the curved diffuser channels complicate the diffuser flow field, making a detailed analysis close to impossible, by the current visualization technique.

Figure 3.5 in Section 3.3, illustrates the diffuser flow during surging at the following condition, 1200 rpm and 70% q^* , for increasing GVFs. In correspondence with the impeller flow, the increase of GVF, leads to an increased bubble number and size accordingly.

The recirculation zone is visible already at very low gas fractions and becomes more distinctive with respect to increasing GVF. An overall view of the diffuser flow mechanisms is given in Figure 6.10a.

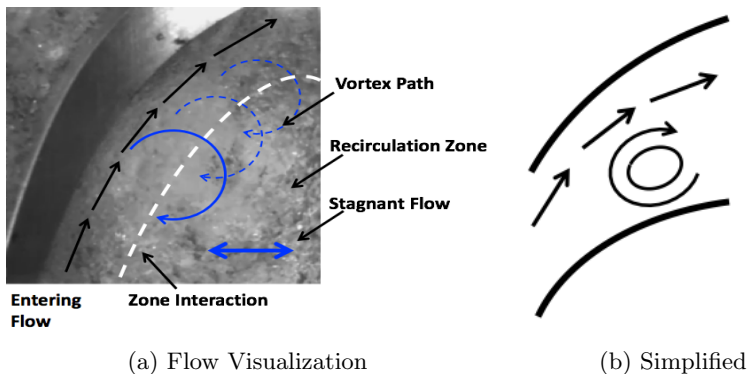


Figure 6.10: Diffuser Channel at Surging: 1800 rpm, 10% GVF and 50% q^*

Figure 6.10b shows a simplified picture of the diffuser flow in Figure 6.10a. In order to reduce the diffuser losses, thin boundary layers as well as high turbulence levels are favourable. The turbulence level affects the exchange of momentum between the boundary layer flow and the main flow, contributing to an improved phase mixing which results in a more stable discharge flow [25]. Thin boundary layers are suitable due to low friction losses, allowing higher flow rates pass through the channels, leading to higher discharge pressure. The interaction line (white dashed line) in Figure 6.10a indicates a threshold between the curved flow and the recirculation zone. The position

of the threshold line is strongly dependent of the operating condition. At the surging onset, flow visualization displays a stagnant zone located at the bottom right region in Figure 6.10a to be moving forth and back obstructing the incoming flow.

Figure 6.11 shows the pressure signals across the diffuser channel synchronized with flow visualization. The red curves represent the diffuser inlet and the green curve shows the diffuser outlet static pressure data.

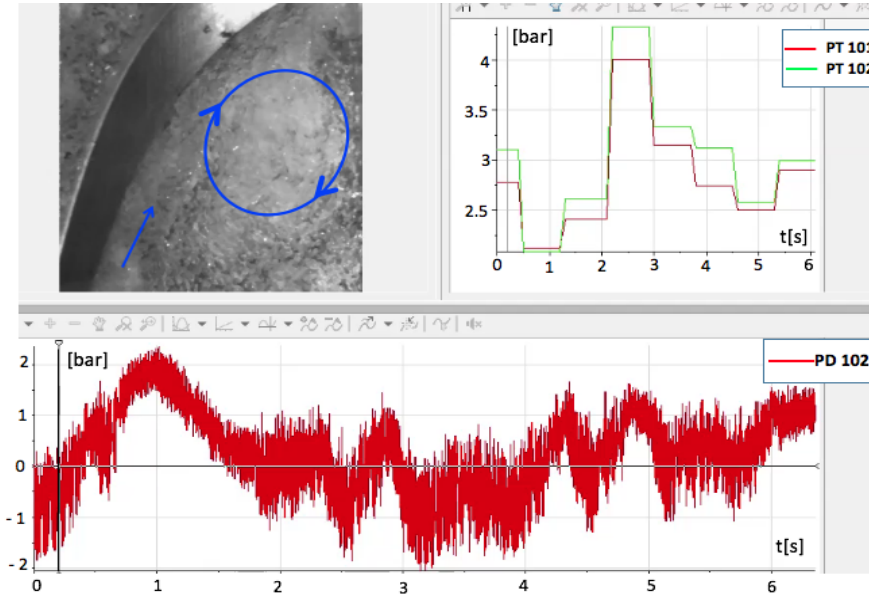


Figure 6.11: Data processing at 1800 rpm, 10% GVF and 50% q^*

The blue circulating arrow indicates the vortices observed during unsteady machine operation. Its clockwise rotation is shown the blue circulation arrow towards the diffuser outlet. The vortex reminds of sudden jets (blue circles in Figure 6.10a) propagating through the diffuser channel. As surging is approached, the jets are observed more frequently, and even with a cyclic occurrence in particular cases. The white color and the low transparency indicate that the vortices and recirculation zone are dominated by breaking gas bubble due to the high phase interaction.

The dynamic pressure signal is seen of the red curve in Figure 6.11, showing significant pressure variations versus time, here with a maximum amplitude of 2 bar. Similar to the empty-of-gas channels, there data processing shows increasing pressure oscillations with respect to increasing rotational speed.

The diffuser is obviously an important part of the pump. In general, the overall diffuser flow field is composed by two main regions, respectively, the curvature flow and the recirculation flow. The recirculation zone proves

to influence the unsteady flow behavior by the stagnant behavior blocking the incoming flow. Fast propagating vortices have been observed by flow visualization. This together with the data processing, led to a potential hypothesis, namely, if the vortices arise as a consequence of the high flow field fluctuations induced by the empty-of-gas channel phenomenon. The correspondence should be considered in terms of further investigations on the intersection region between impeller and diffuser.

6.2 Surging Detection

Major production and economical consequences are associated with surging and machine breakdown. With regards to subsea installations in particular, the systems should be redundant in order to avoid operation failure. The pump must be capable of long term stability and tolerant being exposed to large variations of flow rates and compositions. A successful implementation would require systems preventing critical instabilities. Anti-surge systems for compressors are well known to the industry, but more knowledge is needed in order to develop reliable detection systems for multiphase pumping.

The surging condition has been approached systematically through an extensive test campaign order to detect the inception. It should be noted that the experimental results are highly dependent on the specific semi-axial pump design and set-up. The data is acquired due to the International Organization for Standardization (ISO) 9906 and the permissible uncertainties reported in [2].

6.2.1 Fundamental Variables

The measurements are acquired through a data acquisition system providing signal conditioning through LabVIEW. Test data is logged for intervals of 15, 30, or 60 seconds depending on the specific operating condition. Longer logging time corresponds with increasing instability of the operating condition. Furthermore, the data is processed in order to calculate average and standard deviation values.

Fundamental variables used in the plots are presented below.

Volumetric flow rate relative to the nominal flow rate:

$$q^* = \frac{q_{TP}}{q_{nom}} [\%] \quad (6.1)$$

Discharge pressure variation relative to the average pressure:

$$\delta_p = \frac{p_{3,max} - p_{3,min}}{p_{3,avg}} [\%] \quad (6.2)$$

6.2.2 Surging Detection

Detecting of surging is obviously a challenging task. How to describe and define surging in a multiphase pump vary with the author [30, 40, 1]. The discharge pressure is chosen as a reference value due to the highest variations compared to the other two pressure zones (impeller inlet and outlet).

Table 6.1: Maximum pressure oscillation at surging relative to the respective average pressure

Component	δ_p [%]
Impeller	25.8
Diffuser	62.3
Pump Stage	28.7

The discharge pressure is of high interest due to real operation purposes, due to assure a continuous flow and a certain head to the components downstream. As surging is approached, there follows unwanted flow fluctuations inducing heavy thrust forces in the pump system. In addition to the high variations in pressure, the phenomenon is also recognized from an eye view perspective. The flow field is observed as an "flickering" white annular structure moving back and forth, through the pump channels. In addition, the fluctuations are noticed by the intensified noise and system vibrations. Figure 6.12 pictures the flow fluctuations.

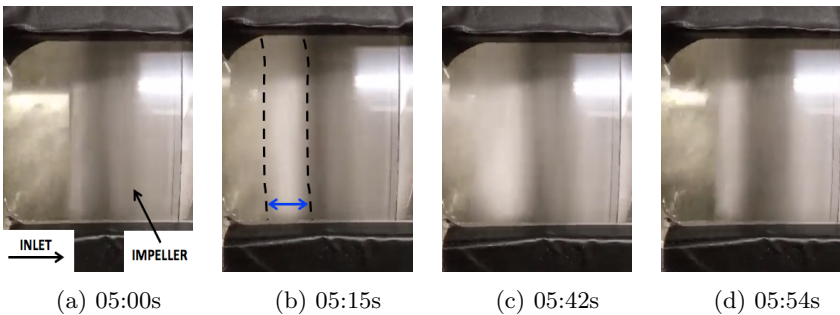


Figure 6.12: Flow fluctuations propagating back and forth within the pump

The images represent a sequence within 50ms showing the distinctive variations at the impeller inlet section. By increasing the GVF, these fluctuations appear more often which is associated with a highly unsteady operating condition.

Figure 6.13 shows the performance curves as a function of relative flow rate at 1800 rpm. The curves in the background indicate the performance curves for gas volume fractions between 0% (single phase) and 20%. Here, the y-axis and x-axis represent the pressure difference across the pump and volumetric flow rate, respectively.

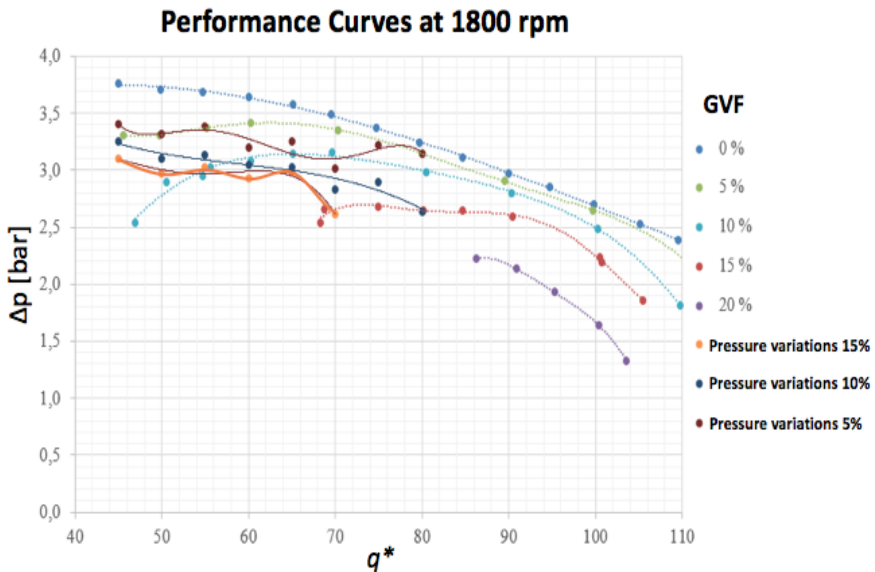


Figure 6.13: Performance curves approaching surging

In general, the background curves show a stable pressure delivery when operating at flow rates close to nominal condition ($q^* = 100\%$). Furthermore, when reducing the volumetric flow rate the background curves become more horizontal shaped, indicating a decreasing pump capability due to changes in flow rate and GVF. Next, as demonstrated of the background curves, the operating capacity reduces with the increasing GVF, accordingly.

The flow rates between 50% and 80% have been studied extensively in order to document the surging inception zone. The outlined curves in Figure 6.13 consider the discharge pressure variations of 5%, 10% and 15%. Consequently, the flow conditions are associated with two main trends: (1) The discharge pressure experiences progressively higher oscillations with increasing GVF, (2) The overall pressure across the pump decreases at higher GVFs.

The pressure data analysis reveals an instability zone due to the sudden increase of pressure variations δ_p . As outlined in Table 6.1, the flow field behavior yields for the whole pump stage, but the strongest pressure deviations are however localized at the discharge pressure. Figure 6.14 and 6.15

show the discharge pressure variations relative to the average pressure, under the following conditions; relative flow rate 70%, 60%, and 50% q^* versus increasing GVF. Each trend line consider a constant volumetric flow rate and rotational speed. Additionally, the figures below show a horizontal line marking the criterion of surging inception.

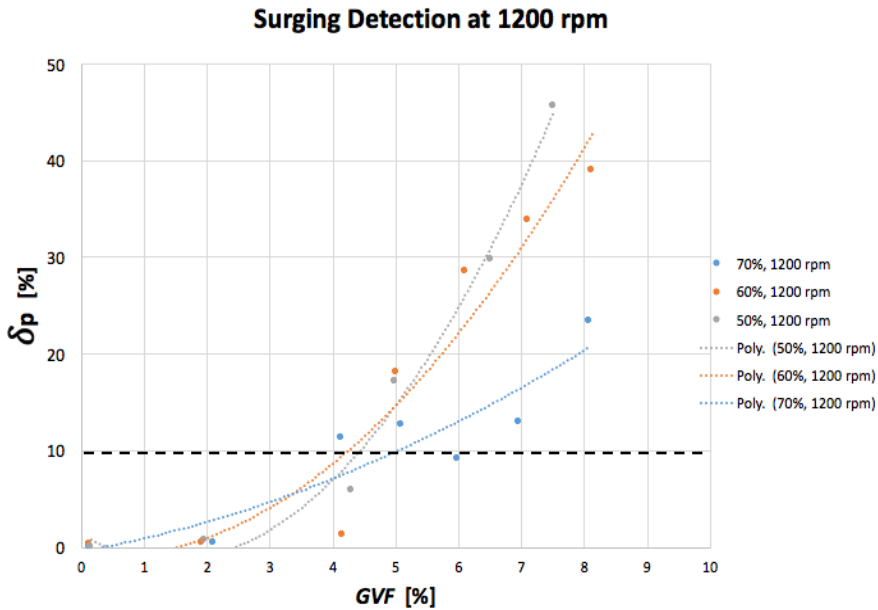


Figure 6.14: Surging inception at partload and 1200 rpm

The trend lines are plotted against the GVF and show a rapid increase of the discharge pressure variations as they intersect the horizontal threshold. The surging detection criterion corresponds with the following definition:

The multiphase pump surging inception is defined as an unsteady operating point of the downstream maximum pressure variations exceeding a threshold of 10% due to the average pressure.

As presented in Section 6.1, surging is associated with complex two-phase flow phenomena. Some of them are; gas pockets, empty-of-gas channels, phase separation, accompanied with strong flow field fluctuations. In general, the curves show a steady behavior for low GVFs, and flow rates close to the nominal flow rate. As the GVF is further increased, the curves are, eventually, seen to increase rapidly in the vertical direction. Accordingly, the curves are seen to increase faster at lower relative flow rates in terms of stronger channel obstructions. This agrees with the flow visualization, where empty-of-gas channels and gas pockets are observed to be more distinctive at lower relative flow rates.

Additionally, Figure 6.15 identifies that the operating conditions at the same

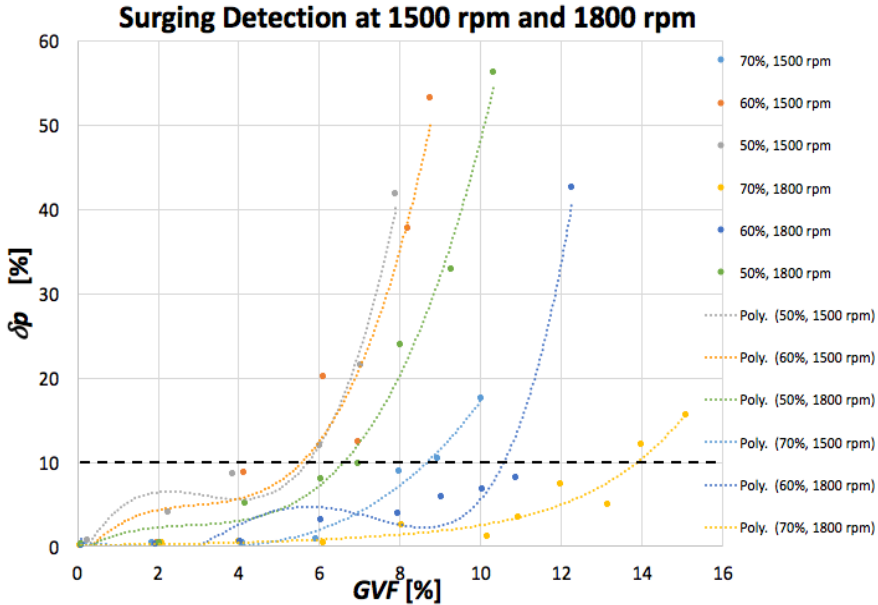


Figure 6.15: Surging inception at partload and 1500 rpm, 1800 rpm

relative flow rate, but lower rotational speed, will exceed the threshold line at lower GVF. This corresponds with the increasing pump capability according to higher rotational speeds, assumed that other parameters are maintained constant.

The exact physical influence of the phase slip is difficult to give due to the absence of necessary measurement techniques and analytical validation of the experimental data. By approaching the surging zone, the flow pattern changes, consequently, from a dispersed flow towards a flow with higher tendencies of phase separation. Eventually, gas-locking will occur and the flow pattern becomes annular (high superficial gas velocity). Regarding the flow pattern transition and the two-phase flow pattern fundamentals [36], the superficial phase velocity and phase slip will change accordingly. The slip can thus be associated with the unstable zone of operation, affecting both the system stability and performance negatively.

6.2.3 Multiphase Booster Surging Zone

As with compressors, the multiphase booster successful operation shows to be limited. Surging inception is recognized by a rapid intensification of the overall flow instabilities. The pump shows to be sensitive to further increase of the GVF or liquid flow deceleration. Furthermore, this section introduces the last possible operating condition, termed "deep surging", which denotes

a severe version of classic surging, which is more difficult to recover from. This term is also used in the literature for turbo compressors (de Jager [13]), where strong axial pulsations and reversal flow is possible. However, reversal flow has not been observed during the experiments.

The data collection accompanied with the detection criterion indicate the surging inception for this specific application. Figure 6.16 shows the surging inception, as well as the deep surging conditions. The data points are chosen from three different rotational speeds at 70%, 60% and 50% q^* with respect to the detection criterion. The x- and y-axis show, respectively, the volumetric flow rate and differential pressure across the pump stage. It should be noted that the volumetric flow rate will vary slightly between the respective surging inception and deep surging (DS) points due to the high flow irregularities.

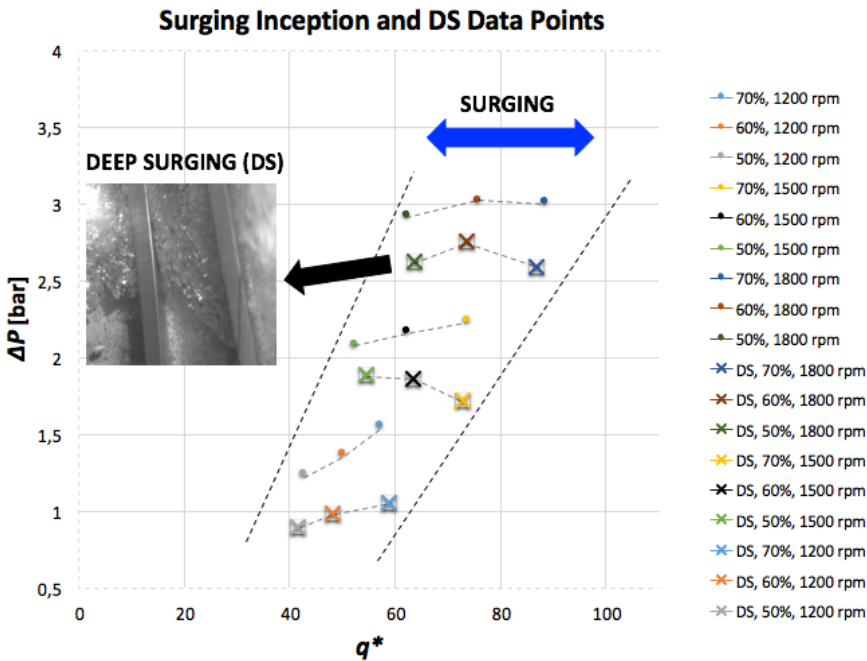


Figure 6.16: Data points showing surging inception (dot point) and deep surging (cross point) conditions

The marked surging zone in Figure 6.16 indicates an unstable operating zone for 50% and 70% q^* , dependent on the gas volume fraction and rotational speed. Figure 6.16 shows a substantial difference between the differential pressure over the pump stage for 1200 rpm, 1500 rpm and 1800 rpm. Moreover, the multiphase booster provides a consistently lower pressure at the deep surging conditions compared to the surging inception. The lower pressure across the pump corresponds with the higher pressure variations. Ad-

ditionally, the specific flow phenomena presented in Section 6.1) have been observed within this unsteady zone of operation.

The surging inception data points are based on the detection criterion according to the variations in GVF. Furthermore, the deep surging condition can be associated with the steep increase of the pressure variations represented in Figure 6.14 and 6.15. The image in Figure 6.16 shows a fully separated flow in the impeller channel, indicating that phase slip and phase separation in the impeller channel. In addition, this operating condition indicates a high risk of gas-locking.

6.3 Summary

The machine operation and multiphase flow characteristics are highly dependent on the operating parameters; GVF, flow rate, and rotational speed. Furthermore, the pump shows an overall reduced capability at low flow rates and high GVFs, characterized by a reduced pressure production across the pump and higher risk of phase separation. Empty-of-gas channels, bubble coalescence, gas pockets, and recirculation zones have shown to play a major role influencing the surging inception and evolution. The latter is mainly observed in the diffuser channels and appears as a stagnant zone, blocking the incoming flow. Furthermore, the recirculation zone is present already at very low gas volume fractions, and becomes more distinct as surging is approached. As a recommendation for improvement, the vane design should be reconsidered and verified with CFD simulations.

Phase separation is a fundamental issue in rotodynamic pumps. With the increase of GVF, it has been observed higher tendencies of coalescing bubbles which further form into gas pockets. Gas pockets are observed both at the pump inlet and inside the impeller channels, with varying shape, size and location, dependent on the operating condition. In particular cases, there have been observed a regular sequence of one flow phenomenon leading to another phenomenon. The one where isolated bubbles flow closely gathered towards lower pressure zones, as the blade suction side, and further form a gas pocket (Figure 6.5). This move is assumed to cause unwanted flow obstructions. Furthermore, the experimental work indicates that such obstructions cause liquid to accumulate, until the pump manages to recover, identified with a following empty-of-gas channel. This sequence is also associated with the last possible operating condition, also termed deep surging, where the pump is highly sensitive to flow changes.

The acquired data and visualization prove these flow phenomena to intensify, as surging is approached. Furthermore, this observation together with the discharge pressure variation, lay the foundation for the detection criterion of surging inception. The criterion is presented of the following definition:

The multiphase pump surging inception is defined as an unsteady operating point of the downstream maximum pressure variations exceeding a threshold of 10% due to the average pressure.

An extensive test campaign should be conducted in order to verify the instability zone criterion. A reliable detection method would require knowledge of all operating conditions. Also, a more fundamental understanding of the physical mechanisms and how they affect the system stability is essential in order to avoid unwanted production regimes in the compression system.

Chapter 7

Conclusion

Due to the complex nature of two-phase fluid mechanics, documenting instabilities and surging mechanisms related to the multiphase booster have shown to be a challenging task. However, the conducted test campaign accompanied with flow visualization and data processing have given an improved insight of the unsteady zone of operation.

Experimental work has resulted in a broad data collection and a quantitative method to detect the surging inception for this specific application. A correspondence between the intensifying overall flow instabilities subject to increasing GVF, has revealed a zone of rapid increasing discharge pressure variations. Consequently, the surging inception is defined as an unsteady operating point of the downstream maximum pressure variations exceeding a threshold value of 10% of the average pressure. The criterion should be supported by further analysis of torque and system vibrations.

Flow visualization accompanied with the available data processing system, have assessed a deeper understanding of specific flow phenomena and trends during the unsteady machine operation. Empty-of-gas channels, phase separation, bubble coalescence, gas pockets and recirculation zones have shown to be the most significant occurring phenomena. The instabilities have shown to intensify as the surging onset is approached, affecting the pressure across the pump as well as the system stability. However, the exact physical mechanisms still remain to be obtained. More advanced visualization and measurement techniques should be considered to support these observations. Laser Doppler velocimetry and particle image velocimetry, accompanied with CFD simulations promise to give a more complete flow field analysis.

The study of phase slip in a rotodynamic multiphase pump has shown to be in an early stage, based on the conducted literature review. Observations of flow visualization at partload operation show higher relative phase slip is corresponds with increasing GVF, as well as with reducing the flow

rate. Furthermore, this thesis has explored the phenomenon through bubble tracking at the impeller inlet region. The bubble shape is maintained by various influencing forces, where the body force and drag force induced by the impeller shows to be the most important ones. Also, when operating at surging, the presence of channel obstructions show to influence the bubble shape by a consecutive flow field deceleration and acceleration. Furthermore, the bubble behavior analysis shows to be important with regards to improvements of computational algorithms and two-phase modeling.

In light of the experimental results, the multiphase booster instability and surging characteristics arise from an increased overall unsteadiness depending on a product of multiple parameters. Further investigations must be conducted in order to understand the unwanted flow conditions.

Chapter 8

Recommended Work in Future Research

Multiphase pump instability and surging is an important field of research due to efficient oil and gas production. During the work of this thesis several areas have emerged to be without answers found in the open literature, which indicates that further research should be performed. The basis for all science research and development is to identify the problems and asking the necessary questions. Further work is required in order to understand the fundamentals and thus lay be able to perform design improvements.

- The MultiBooster test rig at NTNU gives a unique opportunity of flow visualization due to its 360° transparent pump shroud. More advanced visualization techniques such as LVD and PIV would permit a more complete analysis of the flow field. This involves a closer study of the flow mechanisms in terms of surging inception and evolution. These visualization techniques would also be of great value in order to perform a bubble size distribution analysis.
- Documentation and assessment of the phase slip has come out to be a very complex task. A more fundamental understanding of phenomenon would require more advanced measurement tools providing phase velocity and density measurements. Available phase slip correlations are very limited for this type of application. Effort should here be performed in order to assess suitable phase slip correlations, also applicable to unsteady machine operation.
- CFD-analysis should be employed to verify the experimental results in this thesis.
- The thesis test campaign should be conducted again, but this time with a shrouded impeller. This would allow to study the tip leakage

flow influence on the surging inception and evolution, also evaluate the hypothesis of improved phase mixing due to tip leakage flow.

- An extensive test campaign should be conducted in order to document all surging inception conditions. Furthermore, the acquired data collection, accompanied with flow visualization and CFD should be employed to develop a complete surging detection model, applicable for real processing systems.
- The detection criterion for surging inception presented in this thesis should be supported by a time-frequency fast Fourier transformation "FFT" analysis of the system vibrations.

Bibliography

- [1] Serena A. and Bakken L.E. Investigation of the blade tip clearance effects on performance and stability of a mixed-flow pump: High speed camera recordings of the flow structures, local measurements and numerical simulation. 2015.
- [2] Serena A. and Bakken L.E. Design of a multiphase pump test laboratory allowing to perform flow visualization and instability analysis. 2015.
- [3] Serena A. and Bakken L.E. Experimental characterization of the flow instabilities of a mixed-flow multiphase pump operating air and water through local visualization and analysis of dynamic measurements. 2015.
- [4] Patel B. R. and Runstadler P. W. Investigations into the two-phase behavior of centrifugal pumps. *Proceedings of Polyphase Flow in Turbomachinery*, 1978.
- [5] Bratu C. Rotodynamic two-phase pump performances. *Proceedings of SPE annual technical conference and exhibition*, pages 555–567, 1994.
- [6] Pérez C. and Abraham Acuña. *Measurement Techniques to Characterize Bubble Motion in Swarms*. PhD thesis, McGill University, Montreal, Canada, 2007.
- [7] Brennen C. E. *Fundamentals of multiphase flow*. Cambridge University Press, 2005.
- [8] Homer C.J. Theoretical studies of pump performance in two-phase flow. In *European Two-phase Flow Group Meeting, Marchwood*, 1985.
- [9] Sun D. and Prado M. G. Modeling gas-liquid head performance of electrical submersible pumps. *Journal of pressure vessel technology*, pages 31–38, 2005.
- [10] Hellmann D. H. Pumps for multiphase boosting. In *Proc. 2nd Int. Conference on Pumps and Fans*, pages 43–46, 1995.

-
- [11] Cheng Da-Chuan and Burkhardt H. Bubble tracking in image sequences. *International Journal of Thermal Sciences*, pages 647–655, 2003.
- [12] Cheng Da-Chuan and Burkhardt H. Template-based bubble identification and tracking in image sequences. *International Journal of Thermal Sciences*, pages 321–330, 2006.
- [13] Bram De Jager. Rotating stall and surge control: A survey. pages 1857–1862, 1995.
- [14] Barrios L. et al. Cfd modeling inside an electrical submersible pump in two-phase flow condition. pages 457–469, 2009.
- [15] Clift R. et al. *Bubbles, drops, and particles*. Courier Corporation, 2005.
- [16] Falcimaigne J. et al. Multiphase pumping: achievements and perspectives. *Oil & Gas Science and Technology*, pages 99–107, 2002.
- [17] Gaard S. et al. Two-fluid modelling of bubble flow in a mixed-flow pump-impeller. *SINTEF Fluid Machinery, Trondheim, Norway*, pages 156–167, 1991.
- [18] Gamboa J. et al. Experimental study of two-phase performance of an electric-submersible-pump stage. *SPE Production & Operations*, pages 414–421, 2012.
- [19] Gamboa J. A. et al. Review on esp surging correlations and models. In *SPE Production and Operations Symposium*. Society of Petroleum Engineers, 2011.
- [20] Honkanen M. et al. Recognition of highly overlapping ellipse-like bubble images. *Measurement Science and Technology*, page 1760, 2005.
- [21] Lastra R. et al. Feasibility study on application of multiphase pumping towards zero gas flaring in nigeria. 2005.
- [22] Zhang J. et al. Visualization study of gas–liquid two-phase flow patterns inside a three-stage rotodynamic multiphase pump. *Experimental Thermal and Fluid Science*, pages 125–138, 2016.
- [23] Jakobsen H. A. Chemical reactor modeling. *Multiphase Reactive Flows, Berlin, Germany: Springer-Verlag*, 2008.
- [24] Duran J., Prado M. G., et al. Esp stages air-water two-phase performance-modeling and experimental data. 2003.
- [25] Güllich J. F. *Centrifugal pumps*. Springer, 2008.
- [26] Lea J. F. and Bearden J. L. Effect of gaseous fluids on submersible pump performance. *Journal of Petroleum Technology*, 1982.

- [27] Minemura K. and Murakami M. A theoretical study on air bubble motion in a centrifugal pump impeller. *Journal of Fluids Engineering*, pages 446–453, 1980.
- [28] Minemura K. and Uchiyama T. Three-dimensional calculation of air-water two-phase flow in centrifugal pump impeller based on a bubbly flow model. pages 766–771, 1993.
- [29] Barrios L. J. *Visualization and modeling of multiphase performance inside an electrical submersible pump*. 2007.
- [30] Barrios L. J and Prado M. G. Experimental visualization of two-phase flow inside an electrical submersible pump stage. pages 453–467, 2011.
- [31] Barrios L. J. and Prado M.G. Modeling two-phase flow inside an electrical submersible pump stage. *Journal of Energy Resources Technology*, 2011.
- [32] Ishii M. and Mishima K. Two-fluid model and hydrodynamic constitutive relations. *Nuclear Engineering and Design*, pages 107–126, 1984.
- [33] Murakami M. and Minemura K. Effects of entrained air on the performance of a centrifugal pump : 1st report, performance and flow conditions. *Bulletin of JSME*, pages 1047–1055, 1974.
- [34] Prado M. Solid sphere in rotating flow, note lecture. *The University of Tulsa*, 2005.
- [35] Uchiyama T. Minemura, K. Prediction of pump performance under air-water two-phase flow based on a bubbly flow model. *Journal of fluids engineering*, pages 781–783, 1993.
- [36] Bratland O. Pipe flow 2: Multi-phase flow assurance. 2010.
- [37] Furuya O. An analytical model for prediction of two-phase (noncondensable) flow pump performance. *Journal of Fluids Engineering*, pages 139–147, 1985.
- [38] Li Q. and Xue D. Phase separation inside a rotodynamic multiphase pump. *J. University of Petroleum China (Natural Science Edition)*, pages 53–56, 1997.
- [39] Sachdeva R. Two-phase flow through electric submersible pumps, 1990.
- [40] Ramberg R. M. *Multiphase pump performance modelling. PhD thesis*. Norwegian University of Science and Technology, Department of Energy and Process Engineering, Trondheim, 2007.
- [41] Gaard S. Modeling of two-phase bubble flow in centrifugal pumps. *Dr.ing. thesis, Norwegian University of Science and Technology, Trondheim, Norway*, 1992.

-
- [42] ÖZDEMİR S. *Investigation of Air Bubble Motion in Water Through a Vertical Narrow Rectangular Channel by Using Image Processing Techniques*. PhD thesis, Ankara: Middle East Technical University, 2005.
- [43] Grüner T. G. Wet gas compression: Experimental investigation of the aerodynamics within a centrifugal compressor exposed to wet gas. 2012.
- [44] Estevam V. Uma análise fenomenológica da operação de bomba centrífuga com escoamento bifásico. *Universidade Estadual de Campinas, Faculdade de Engenharia Mecânica*, 2002.

Appendices

A P&ID & Instrumentation List

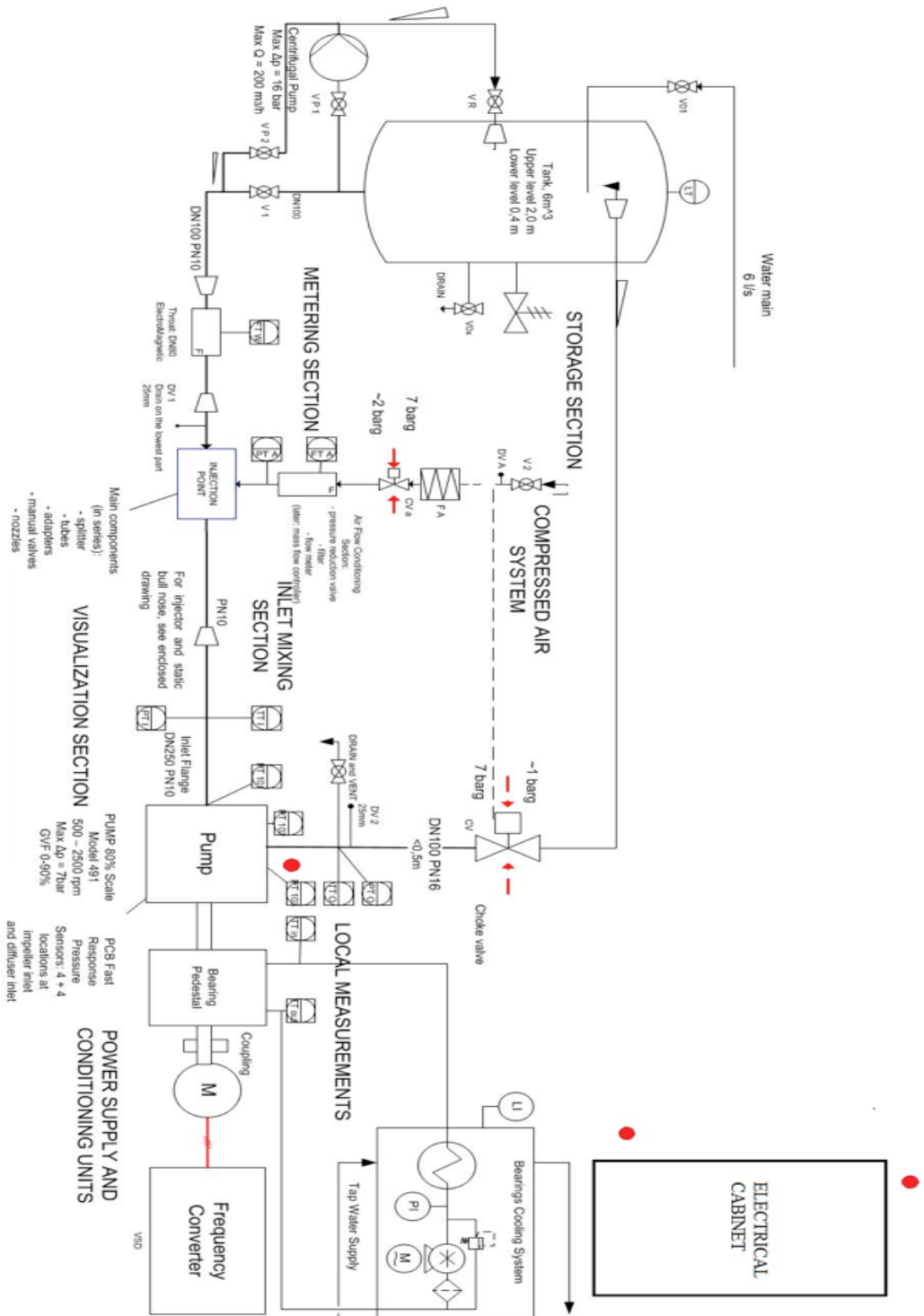


Figure 1: P&ID

Instrumentation List:

Tag-ID	Sensor type	Mfc.	Model	Range min	Range max	Signal		
PT101	Pressure Transmitter	Aplisens	PCE-28 Smart	0 bar(a)	7 bar(a)	AI	4-20 mA	two-wired signal
PT102	Pressure Transmitter	Aplisens	PCE-28 Smart	0	7	AI	4-20 mA	two-wired signal
PT103	Pressure Transmitter	Aplisens	PCE-28 Smart	0	7	AI	4-20 mA	two-wired signal
PT I	Pressure Transmitter	Aplisens	PCE-28	0	2	AI	4-20 mA	two-wired signal
PT A	Pressure Transmitter	Aplisens	PCE-28	0 bar(g)	7 bar(g)	AI	4-20 mA	two-wired signal
PT O	Pressure Transmitter	Aplisens	PCE-28	0 bar(g)	7 bar(g)	AI	4-20 mA	two-wired signal
TT I	Temperature Transmitter	Aplisens	CT 14	0	60	AI	4-20 mA	two-wired signal
TT O	Temperature Transmitter	Aplisens	CT 14	0	60	AI	4-20 mA	two-wired signal
CV	Choke Valve	Flowserve	Logix 510 si			AO/AI		
FTA	Flow Meter	Bronkhorst		0	200 m ³ /h	AI	4-20 mA	current
FTW	Flow Meter	ABB	FEV112	0	200Nm ³ /h	AI	4-20 mA	
VSD	Variable Speed Drive	Lonne				AO	4-20 mA	

Figure 2: Instrumentation list

B Graphs

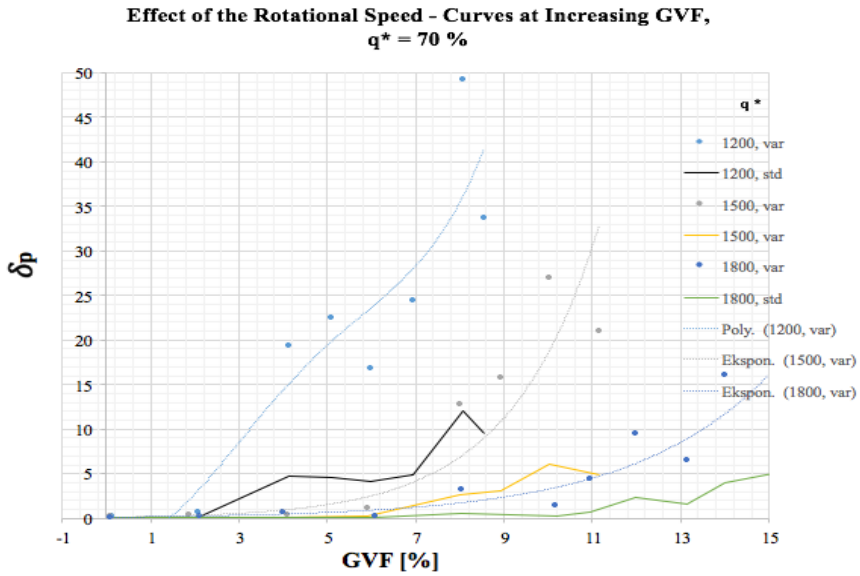


Figure 3: Surging detection

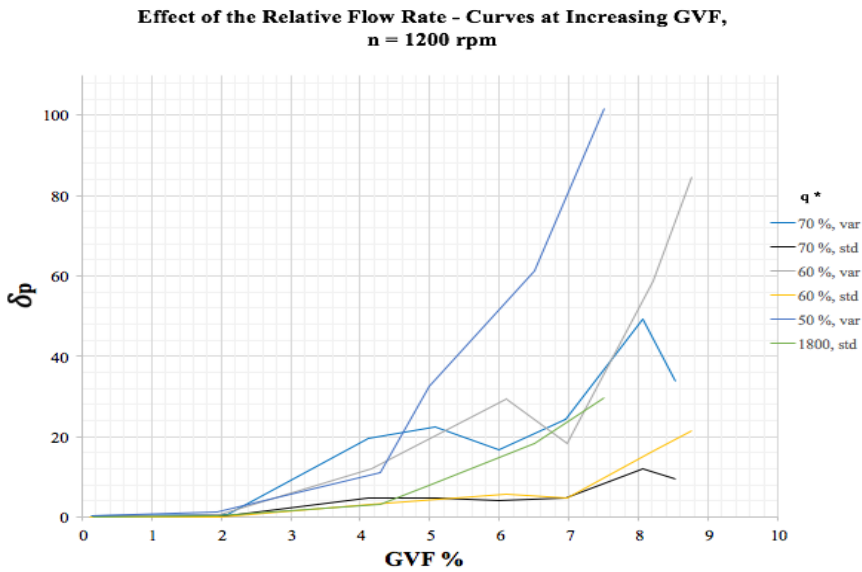


Figure 4: Surging detection

C Phase slip correlations for 1D pipe flow

The equations presented in this appendix are based on NTNU lecture notes in multiphase pipe flow from Ole Jørgen Nydal.

Phase slip correlations for bubbly flow by Malnes, Bankoff and Zuber-Findlay:

Malnes bases the phase velocity through slip and relative average velocity on gas velocity:

Slip ratio:

$$S_M = C_M \left(1 + \frac{U_{rM}}{U_l} \right) \quad (1)$$

where:

$$U_{rM} = \frac{\int (1-\alpha) u_r}{\int (1-\alpha)}$$

$$U_g = C_M (U_l + U_{rM}) \quad (2)$$

where:

$$C_M = \frac{1-\alpha}{D-\alpha},$$

$$\text{and } \frac{1}{D} = \frac{A \int \alpha u_g}{\int \alpha \int u_g}$$

Bankoff used the same procedure as Malnes, but with a correlation based on liquid velocity instead of gas velocity:

$$U_g = C_B U_l + U_{rB} \quad (3)$$

where:

$$C_B = \frac{1-\alpha}{K-\alpha},$$

$$\frac{1}{K} = \frac{A \int \alpha u_l}{\int \alpha \int u_l}$$

Zuber-Findlay:

$$U_g = C_{ZF} * U_m + U_{gj} \quad (4)$$

where:

$$C_{ZF} = \frac{A \int \alpha u_m}{\int \alpha \int u_m},$$

$$U_{gj} = \frac{\int \alpha u_{gj} dA}{\int \alpha dA} \text{ (average drift flux).}$$

D Bubble Tracking



Figure 5: Bubble Tracking

E Gantt Diagram

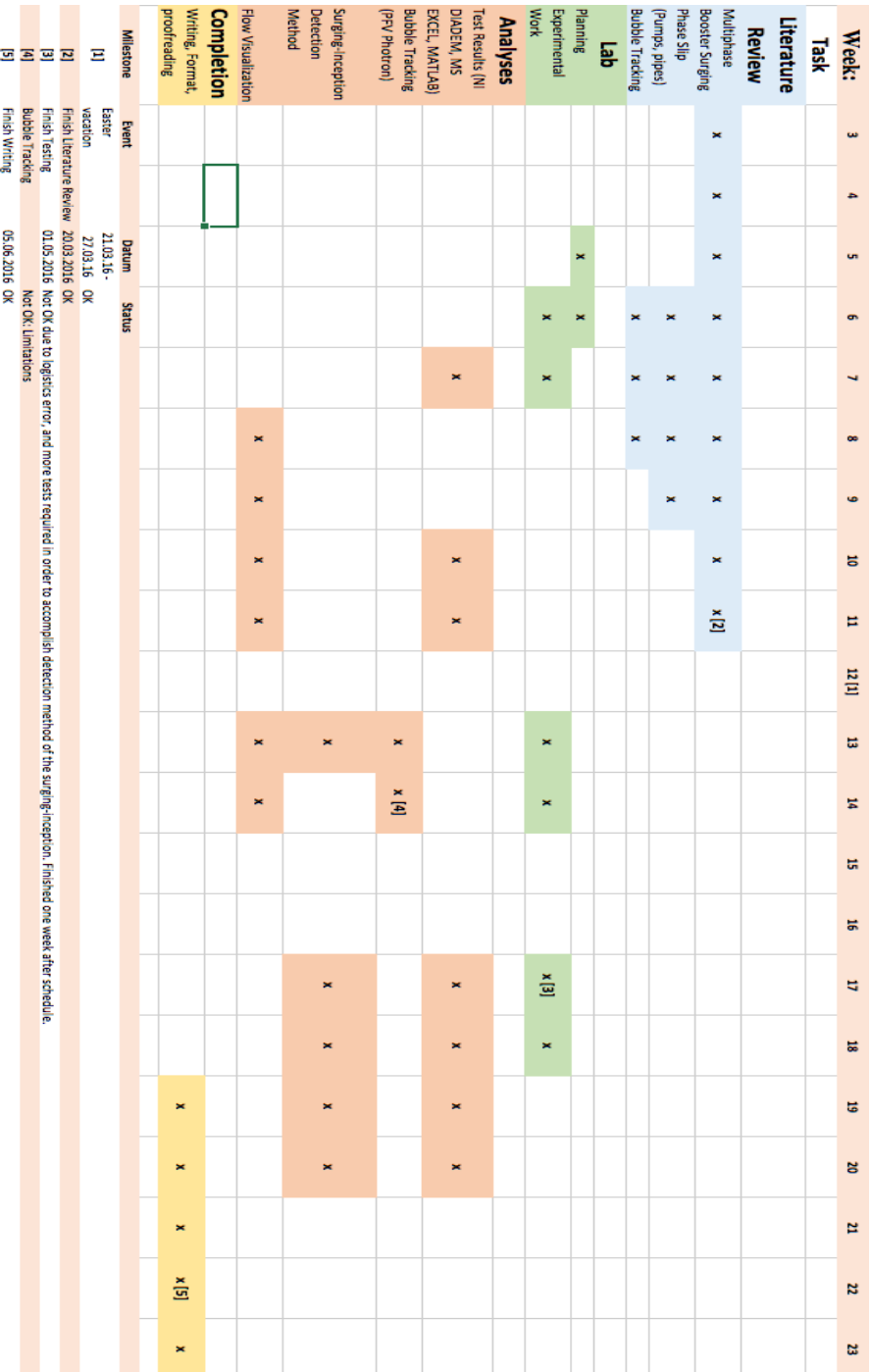


Figure 6: Gantt Diagram – Master Thesis